

LARGE-SCALE BIOLOGY ARTICLE

The Systems Architecture of Molecular Memory in Poplar after Abiotic Stress

Elisabeth Georgii¹, Karl Kugler², Matthias Pfeifer², Elisa Vanzo³, Katja Block³, Malgorzata A. Domagalska⁴, Werner Jud^{3,6}, Hamada AbdElgawad^{4,8}, Han Asard⁴, Richard Reinhardt⁵, Armin Hansel⁶, Manuel Spannagl², Anton R. Schäffner¹, Klaus Palme⁷, Klaus F.X. Mayer^{2,9*}, Jörg-Peter Schnitzler^{3*}

¹ Institute of Biochemical Plant Pathology, Helmholtz Zentrum München, German Research Center for Environmental Health, 85764 Neuherberg, Germany.

² Plant Genome and Systems Biology, Helmholtz Zentrum München, German Research Center for Environmental Health, 85764 Neuherberg, Germany.

³ Research Unit Environmental Simulation, Institute of Biochemical Plant Pathology, Helmholtz Zentrum München, German Research Center for Environmental Health, 85764 Neuherberg, Germany.

⁴ Laboratory for Integrated Molecular Plant Research, University of Antwerp, 2020 Antwerp, Belgium.

⁵ Max Planck Genome Centre Cologne, Max Planck Institute for Plant Breeding Research, 50829 Köln, Germany.

⁶ Institute for Ion Physics and Applied Physics, University of Innsbruck, 6020 Innsbruck, Austria.

⁷ Institute of Biology II/Molecular Plant Physiology, Faculty of Biology, BIOS Centre for Biological Signalling Studies, Centre for Biological Systems Analysis, 79104 Freiburg, Germany.

⁸ Botany and Microbiology Department, Faculty of Science, Beni-Suef University, Beni-Suef, Egypt.

⁹ TUM School of Life Sciences, Technical University Munich, Weihenstephan, Germany.

*Corresponding Authors: jp.schnitzler@helmholtz-muenchen.de; k.mayer@helmholtz-muenchen.de.

Short title: Systems architecture of molecular memory

One-sentence summary: The transcriptomic memory in poplar trees after recovery from drought-heat stress changes with stress frequency and intensity and involves a complex interplay of common and tissue-specific factors.

The authors responsible for distribution of materials integral to the findings presented in this article in accordance with the policy described in the Instructions for Authors (www.plantcell.org) are: Jörg-Peter Schnitzler (jp.schnitzler@helmholtz-muenchen.de) and Klaus F.X. Mayer (k.mayer@helmholtz-muenchen.de).

ABSTRACT

Throughout the temperate zones, plants face combined drought and heat spells in increasing frequency and intensity. Here, we compared periodic (intermittent, i.e. high-frequency) versus chronic (continuous, i.e. high-intensity) drought-heat stress scenarios in gray poplar (*Populus*

x *canescens*) plants for phenotypic and transcriptomic effects during stress and recovery. Post-recovery photosynthetic productivity after stress exceeded the performance of poplar trees without stress experience. We analyzed the molecular basis of this stress-related memory phenotype and investigated gene expression responses across five major tree compartments including organs and wood tissues. For each of these tissue samples, transcriptomic changes induced by the two stress scenarios were highly similar during the stress phase but strikingly divergent after recovery. Characteristic molecular response patterns were found across tissues but involved different genes in each tissue. Only a small fraction of genes showed similar stress and recovery expression profiles across all tissues, including type 2C protein phosphatases, the LATE EMBRYOGENESIS ABUNDANT PROTEIN4-5 genes, and homologs of the *Arabidopsis thaliana* transcription factor HOMEBOX7. Analysis of the predicted transcription factor regulatory networks for these genes suggested that a complex interplay of common and tissue-specific components contributes to the coordination of post-recovery responses to stress in woody plants.

1 INTRODUCTION

2 Climate change increases the frequency and intensity of extreme events such as heat waves
3 and drought (IPCC, 2014). Plants, particularly long-living trees, have evolved flexible
4 mechanisms to cope with environmental stresses (Harfouche et al., 2014). Poplar (*Populus*
5 spp.) is a widely used model in tree research that combines moderate genome size, a
6 complete genome reference, fast growth, rapid maturation and wide geographic distribution
7 with economic relevance for wood and biomass production (Taylor, 2002; Tuskan et al.,
8 2006). Poplar is also suitable for transcriptome studies across a variety of tissues. For
9 instance, co-expression patterns underlying cambial growth and wood formation have been
10 investigated by sampling multiple sections across tree trunks (Sundell et al., 2017). Various
11 physiological changes have been observed in plants in response to abiotic stresses. Drought
12 limits water uptake by roots and results in reduced transpiration and photosynthesis, which
13 can have severe effects on growth and yield (Aroca et al., 2012; Osakabe et al., 2014). These
14 processes are mediated by well-known molecular responses of cells to drought, frequently
15 triggered by the plant hormone abscisic acid (ABA) (Osakabe et al., 2014; Shinozaki and
16 Yamaguchi-Shinozaki, 2007). In addition to ABA-responsive element-binding (AREB/ABF)
17 transcription factors, members of the no apical meristem, *Arabidopsis thaliana* transcription
18 activation factor and cup-shaped cotyledon (NAC) and dehydration-responsive element-
19 binding (DREB) transcription factor families orchestrate pronounced gene expression
20 changes upon drought stress, as demonstrated in *Arabidopsis* and crop species (Nakashima
21 et al., 2014).

22 Stress exposure also alters gene expression beyond the duration of the stress phase, forming
23 a molecular "memory" (Crisp et al., 2016; Fleita-Soriano and Munne-Bosch, 2016). A well-
24 studied effect of stress-related memory is enhanced tolerance towards subsequent stress
25 events, as reflected by response differences between the first and subsequent stress
26 challenges (Ding et al., 2012; Ding et al., 2013; Liu et al., 2016). This "primed response" is
27 characterized by gene expression changes that induce damage protection, growth regulation,
28 osmotic readjustment and the coordination of hormonal crosstalk (Ding et al., 2013). Such an
29 expression memory can also involve chromatin remodeling through histone modifications
30 (Lämke et al., 2016; Sani et al., 2013). Phenotypically, plants primed by drought stress have
31 shown a higher photosynthesis rate during subsequent stress periods than non-primed plants
32 (Wang et al., 2014). Even in the absence of a further stress challenge, plant performance can
33 have signs of a stress-related memory after successful stress recovery, significantly differing
34 from untreated control plants (Hagedorn et al., 2016; Xu et al., 2010). The molecular basis of
35 this post-recovery phenotype is still largely unexplored.

36 In the present study, we focused on gene expression changes during stress and after
37 recovery in a woody plant species. In particular, we investigated expression characteristics of
38 stress-related memory, which we define in the context of this work as a post-recovery steady
39 state in stress-treated trees that is distinct from that of non-treated trees. Our analysis not
40 only contrasts stress scenarios that differ in frequency and intensity but also compares
41 responses in different tissues of poplar trees. We simulated predicted regional climate
42 conditions (IPCC, 2014) by applying simultaneous drought and heat spells at the elevated
43 atmospheric carbon dioxide (CO₂) concentrations expected in 2050 to explore how gray
44 poplars (*Populus x canescens*) that have recovered from drought-heat stress differ from non-
45 treated plants. We characterized the stress response and the stress-related post-recovery
46 memory regarding leaf photosynthesis phenotypes and transcriptional responses of young
47 ("sink") and mature ("source") leaves (Vanzo et al., 2015), phloem-bark, developing xylem
48 and roots. Two stress scenarios of equal total duration were compared to contrast periodic,
49 intermittent stress (PS) with chronic, continuous stress (CS).

50 The post-recovery effects of abiotic stress we observed at the transcriptome level extend the
51 established concept of a molecular memory after stress exposure. While previous work has
52 analyzed gene expression changes in response to recurrent versus initial stress challenges,
53 our analysis also investigates stress-induced shifts in steady state after recovery, i.e., before

54 a new stress challenge. Still, the aspect of recurrent versus one-time stress is covered by the
55 two stress scenarios, which are compared to control scenarios not only at the end of the
56 stress phase but also after recovery. The multifactorial study sheds light on the regulatory
57 architecture of memory-related gene expression networks after different climatic challenges
58 and across multiple tree organs and tissues.

59

60 **RESULTS**

61 **Impact of drought-heat stress periods on post-recovery photosynthetic performance**

62 To obtain a systems-level view of the stress response and recovery in a woody plant species,
63 we subjected groups of gray poplar (*Populus x canescens*) trees to one of four climate
64 scenarios and collected transcriptome samples from five tree compartments (organs and
65 wood tissues) at two subsequent time points (Figure 1). In addition, we took phenotypic
66 measurements of photosynthesis in attached leaves (Figure 1A). The experiment was
67 performed in climate chambers under highly controlled conditions, including a chronic drought
68 and heat stress scenario at elevated CO₂ levels (CS scenario), a periodic drought and heat
69 stress scenario at elevated CO₂ levels with two intermediate recovery periods (PS scenario),
70 a control scenario at elevated CO₂ levels (EC scenario) and a control scenario at ambient
71 CO₂ levels (AC scenario) (Vanzo et al., 2015). AC represents the current temperate climate
72 as a reference point, which allowed us to estimate the effects of predicted future climate
73 scenarios (EC, CS and PS). The stress phase of 22 days was followed by a recovery period
74 of one week under irrigation and temperature conditions equal to those for control plants (see
75 Methods). Phenotypic photosynthetic performance of mature leaves was assessed using gas
76 exchange measurements (Jud et al., 2016; Vanzo et al., 2015). During the stress phase, the
77 net CO₂ assimilation rate of leaves was significantly reduced for CS-treated poplar trees
78 compared to the corresponding EC control trees (p.adj=0.0347). PS-treated trees showed
79 intermediate levels (Figure 1B). The same response pattern was found for the transpiration
80 rate (Figure 1C) and stomatal conductance (Figure 1D). For all three physiological
81 parameters, AC and EC controls were not significantly different. At the end of the recovery
82 phase, the leaf transpiration rate and stomatal conductance of stress-treated trees reached
83 similar levels to those of the control trees, suggesting that the trees indeed had recovered
84 from the combined drought and heat spells (Figure 1C-D). The recovery of the physiological

85 phenotype is also confirmed by the clear separation between stress phase and recovery
86 measurements for each stress treatment and physiological parameter (Figure 1B-D).
87 Remarkably, the leaf net CO₂ assimilation rates of PS- and CS-treated trees not only
88 recovered but were significantly higher than that of AC trees (p.adj=0.0089 and p.adj=0.0388,
89 respectively), with intermediate levels for EC trees (Figure 1B). Evaluating continuous net
90 ecosystem exchange measurements throughout the entire experiment (Vanzo et al., 2015),
91 both PS- and CS-treatments led to a significant increase in the daily rates of canopy level C
92 gain from photosynthesis during the second half of the recovery phase (days 26 to 29)
93 compared with the control scenarios (Figure 1E).

94

95 **Shared effects between transcriptomic and phenotypic data**

96 We integrated photosynthetic gas exchange data with RNA-seq data from mature leaves by
97 regularized canonical correlation analysis (Le Cao et al., 2009) (see Methods). RNA-seq
98 reads were mapped to the *Populus trichocarpa* reference genome (Sundell et al., 2017;
99 Tuskan et al., 2006). Both data types shared major stress and recovery effects, as reflected
100 by the first and second correlated component, respectively (Figure 1F). For component one,
101 the most representative phenotypic variable is the ratio between net CO₂ assimilation rate
102 and stomatal conductance (Pearson correlation -0.96). The leaf transpiration rate showed a
103 correlation of 0.95 with component one, which is consistent with stomatal closure upon
104 drought stress (Osakabe et al., 2014). The dominating genes for component one also have
105 known stress response functions. Among the top ten genes up-regulated during stress
106 (correlation < -0.95), six genes were annotated as encoding heat shock proteins
107 (Potri.012G022400, Potri.010G195700, Potri.013G089200, Potri.017G130700,
108 Potri.010G088600, Potri.010G053400), potentially acting as chaperones in protein folding.
109 This could indicate a response to elevated leaf temperature caused by heat and a lack of
110 transpirational cooling (Kotak et al., 2007). Indeed, the mean temperature of mature leaves in
111 the experiment increased to more than 35°C during PS and CS, whereas it ranged from 27°C
112 to 30°C after recovery and for the controls (see Figure S4 of Vanzo et al., 2015). Considering
113 all 589 genes that were up-regulated under PS and CS in mature leaves ($\log_2(\text{fold change}) > 1$,
114 p.adj < 0.05; Supplemental Data Set 1), protein folding is also the top enriched Gene Ontology
115 (GO) category (p.adj = 5.64e-9; Supplemental Data Set 2). At the same time, the top down-

116 regulated variables associated with component one included an MYB (myeloblastosis)
117 transcription factor (Potri.002G260000), a peroxidase (Potri.016G132666) and a glutaredoxin
118 gene (Potri.014G134300), indicating changes in transcriptional regulation and stress
119 signaling. Oxidoreductase, peroxidase and transcription factor activity functions were also
120 significantly enriched among the genes down-regulated in mature leaves by both stresses,
121 along with many other processes including protein phosphorylation, cell wall modification,
122 proteolysis, transmembrane transport, cell division and defense response (Supplemental Data
123 Set 3). The recovery phase mature leaf samples were indistinguishable from control samples
124 with respect to component one, suggesting the disappearance of major stress characteristics
125 and thus successful recovery.

126 The second component linking phenotypic and gene expression data points to differences
127 between recovery phase samples and untreated samples (Figure 1F). Component two is
128 characterized by an increased mean net CO₂ assimilation rate in the recovery samples
129 (Pearson correlation 0.77), which is consistent with the results of phenotypic data analysis
130 (Figure 1B). Individual genes did not correlate significantly with component two, and the up-
131 regulated genes shared by both stress treatments after recovery were not enriched for
132 specific functions (Supplemental Data Set 4). Nucleotide binding and ATPase activity for
133 transmembrane movement were enriched among the down-regulated genes of both stress
134 treatments but much more pronounced for CS (Supplemental Data Set 5). PS-specific up-
135 regulation was enriched for stress response genes (e.g. the heat shock protein
136 Potri.004G073600, Supplemental Data Set 4). Many genes were up-regulated only for one
137 stress treatment type; for instance, the putatively photosynthesis-associated plastocyanin-like
138 domain gene Potri.001G332200 was only up-regulated for PS (Supplemental Data Set 1,
139 Figure 2). These results indicate that the post-recovery transcriptomes of PS and CS in
140 mature leaves share more subtle, multivariate effects.

141

142 **Systemic and tissue-specific stress responses**

143 In addition to the mature leaf data described so far, we also obtained RNA-seq
144 measurements from young leaves, phloem-bark, developing xylem and fine roots. This
145 analysis provided a comprehensive systems-level view on the transcriptional responses
146 occurring during stress application and after recovery (Figure 2). To simplify the figure keys

147 and descriptions, the term "tissue" hereafter refers to exactly this set of organs and tissues.
148 The predominant gene expression variation across biological samples was attributable to
149 distinct tissue characteristics (Figure 2A). Whole-tree gene expression profiles concatenating
150 profiles of tissue samples from the same tree clearly separate PS and CS stress phase trees
151 from controls and recovery phase trees (Figure 2B). In all tissues, PS and CS evoked very
152 similar transcriptomic responses relative to EC. For both up- and down-regulated genes
153 ($\text{abs}(\log_2 \text{ fold change}) > 1$, $p.\text{adj} < 0.05$), the observed overlap between the stress types was
154 always larger than one or both of the stress type-specific fractions, suggesting that both
155 scenarios evoke similar molecular stress responses in the tree (Figure 2C, top panel). Among
156 all tissues, the largest overlap between the two stress types was found in the developing
157 xylem, indicating pronounced changes in the upward transport system of the plant.
158 Significantly enriched GO functions ($p.\text{adj} < 0.05$) among the up-regulated genes that overlap
159 between PS and CS xylem samples include oxidoreductase activity, transcription factor
160 activity, transporter activity and response to stress. In the root, genes encoding recognition
161 proteins (e.g. lectin, glycoprotein) and ATPases were activated by both stress types, whereas
162 common stress responses in phloem-bark and leaves were dominated by protein folding
163 processes (Supplemental Data Set 2). In total three genes were found to be up-regulated for
164 each stress scenario in each tissue: Potri.T044100 (one of two co-orthologs of the TCP
165 [TEOSINTE BRANCHED1, CYCLOIDEA, PCF] family transcription factors AT5G41030 and
166 AT3G27010), Potri.008G133200 (one of two co-orthologs of the O-glycosyl hydrolase
167 AT2G01630) and Potri.001G293000 (not annotated). The annotation of genes was taken from
168 the Phytozome portal (Goodstein et al., 2012; Tuskan et al., 2006) throughout this work (see
169 Methods).

170 Regarding the genes down-regulated under both type of stress, the developing xylem showed
171 many enriched processes, such as translation, microtubule-based movement, DNA
172 replication, carbohydrate metabolic process, cell wall, electron transfer activity and
173 transmembrane transport, suggesting a down-regulation of cell division and growth
174 (Supplemental Data Set 3). Similarly, roots showed significant down-regulation of
175 nucleosome, cell wall, electron transfer activity and carbohydrate metabolic process genes.
176 For phloem-bark, we also observed a significant transcriptional decrease in genes involved in
177 cell wall modification, microtubule-based movement and carbohydrate metabolic process. In
178 addition, a strong reduction in the expression of genes involved in proteolysis and response to

179 oxidative stress was found in this tissue. The same was observed for down-regulated genes
180 in young leaves, with an additional enrichment in fatty acid biosynthetic process,
181 transmembrane transport, DNA replication and response to auxin. These results, along with
182 the observations in mature leaves (see above), indicate that both stress treatments (CS and
183 PS) had similar effects, leading to the down-regulation of growth-related processes across all
184 tissues.

185 However, we also found differences between PS and CS. In leaf and root tissues, PS induced
186 more gene expression changes than CS, whereas the CS response was more pronounced
187 than the PS response in xylem and phloem-bark tissues. The PS-specific up-regulated genes
188 detected in root are enriched for ATPases acting as transporters. This up-regulation might be
189 at least partially attributable to priming effects, since PS plants had experienced their third
190 stress phase, whereas CS plants were still in their first stress challenge at day 22 (d22; Figure
191 1A). CS-specific up-regulated genes in developing xylem are enriched for ATPase activity and
192 photosystem II functions. This pattern of up-regulated gene expression is consistent with the
193 previous observation that stem photosynthesis involving the use of internal CO₂ from
194 respiration may play a role in young poplar plants, especially during drought stress (Bloemen
195 et al., 2016), although light penetration through the bark is limited (Pfanzen et al., 2002). The
196 CS-specific up-regulation of photosystem genes may reflect the slightly more severe water
197 deficiency during CS (shoot midday water potential (ψ_{md}) -1.52 ± 0.10 MPa) relative to PS (ψ_{md}
198 -1.27 ± 0.05 MPa) and the controls (EC: ψ_{md} -0.97 ± 0.07 MPa, AC: -0.97 ± 0.04 MPa), increasing
199 the need for C assimilation via a pathway that does not lead to further dehydration promoted
200 by open stomata. CS-specific down-regulated genes in developing xylem are enriched for
201 endoplasmatic reticulum and intracellular protein transport (Supplemental Data Set 3). The
202 gene regulation patterns in the developing xylem illustrate the tissue specificity of stress
203 responses, with a high similarity between periodic and chronic stress as well as stress-
204 specific enhancement of various processes.

205

206 **Post-recovery characteristics of stress-treated trees**

207 After one week of recovery from periodic or chronic stress, respectively, the total number of
208 differentially regulated genes relative to the EC control plants was lower than that at the end
209 of the stress phase across all poplar tissues (Figure 2C). This suggests that the

210 transcriptomes had left the stress state and again approached the state of control plants. The
211 stress recovery was physiologically confirmed by gas exchange (Figure 1C-D) and shoot
212 water potential measurements, which had recovered to -0.72 ± 0.10 MPa and -0.93 ± 0.07 MPa
213 in PS and CS, respectively (compare to previous paragraph; see Methods). In contrast to the
214 stress phase observations, fewer differentially expressed genes were shared between PS and
215 CS than were specifically up- or down-regulated in one of the two stress scenarios (Figure
216 2C, bottom panel). This divergence between stress types during the recovery phase indicates
217 that most stress-activated genes are no longer induced and that the recurrence or duration of
218 drought-heat stress alters the post-recovery processes of plants. In all tissues except mature
219 leaves, PS induced more up-regulated genes during the recovery phase compared to CS.

220 The largest number of up-regulated genes after recovery from PS occurred in young (sink)
221 leaves (Vanzo et al., 2015), followed by mature (source) leaves. In young leaves, the up-
222 regulated genes were dominated by oxidation-reduction, coenzyme binding, hexosyl
223 transferase and carbohydrate metabolic process GO terms (Supplemental Data Set 4). The
224 re-induction of carbohydrate metabolism gene expression after its decrease during stress
225 (see above) indicates that growth processes were reactivated in young leaves. CS-specific
226 expression patterns were characterized by the down-regulation of genes involved in unfolded
227 protein binding, protein folding and response to stress for young leaves and the down-
228 regulation of oxidoreductase activity for phloem, which are indicative of stress recovery
229 (Supplemental Data Set 5). By contrast, for mature leaves of post-recovery trees, PS-specific
230 enrichment indicated the continued activity of several stress response genes, e.g. with
231 functions as heat shock protein (Potri.004G073600) or drought-related late embryogenesis
232 abundant protein (Potri.010G012100). Also, transcription factor genes showed PS-specific
233 transcriptional up-regulation in post-recovery mature leaves, e.g. Potri.006G221500, one of
234 six poplar co-orthologs of Arabidopsis MYB123 involved in anthocyanin and pro-
235 anthocyanidin biosynthesis. In agreement with that finding, anthocyanin levels of poplar
236 leaves at the post-recovery time point were higher for PS than for EC and CS (Vanzo et al.,
237 2015). Genes involved in transporter activity tended to be up-regulated in young leaves
238 ($p_{\text{adj}}=0.06$), including many aquaporin genes (Potri.001G235300, Potri.009G005400,
239 Potri.009G013900, Potri.009G027200), some of which were also up-regulated in other post-
240 recovery tissues (phloem, mature leaves) of PS or CS trees, which could be an indication of
241 drought decline (Supplemental Data Set 1).

242 Biochemical data that monitored the antioxidative system in mature leaves also confirm the
243 recovery from the stressed state (Supplemental Data Set 6), matching the gene expression
244 response profiles (Figure 2C). Leaves of PS-treated trees exhibited a significant decrease in
245 relative reduced ascorbate content during the stress phase ($p_{\text{adj}}=0.0347$), indicating
246 increased scavenging of reactive oxygen species (AbdElgawad et al., 2016). By contrast, all
247 stress-treated and control trees displayed similar levels of relative reduced ascorbate at the
248 end of the recovery phase in leaves (Figure 2D). In addition, we compared the treatment-
249 related expression responses between post-recovery and stress-phase tissue samples to
250 assess how much the molecular processes in each tissue differ between the two phases.
251 Interestingly, the fraction of post-recovery up-regulated genes that already showed up-
252 regulation during the stress phase varied widely among tissues, ranging from 58% in xylem to
253 7% in young leaves for PS and from 69% in xylem to 6% in mature leaves for CS (Figure 2E).
254 This suggests that for some tissues, molecular processes after recovery resemble molecular
255 processes during stress, whereas for other tissues, post-recovery and stress responses are
256 largely different. For instance, ATPases and transport functions played a major role in
257 developing xylem during both phases, whereas for young leaves, genes involved in
258 carbohydrate metabolism were down-regulated during stress (both PS and CS) and up-
259 regulated after recovery.

260 Among different tissues, the gene expression response patterns showed only a slight overlap
261 (Figure 3). During the recovery phase, we did not find any differentially expressed gene that
262 responded across all tissues in PS or CS. Nevertheless, the five tissues shared similar
263 characteristic stress and post-recovery expression profiles involving distinct co-expression
264 modules in each tissue (Figure 4, Methods, Supplemental Data Set 7). Interestingly, more
265 than half of these characteristic profiles exhibited a pronounced difference between stress-
266 exposed plants and non-treated plants at the end of the recovery phase, which is indicative of
267 stress-related memory (Figure 4, bottom). For example, young and mature leaf modules in
268 the memory community C12 included the glutathione-S-transferase gene Potri.019G130566,
269 which protects plants against oxidative damage, and the esterase gene Potri.017G062300,
270 with highest similarity to an Arabidopsis gene involved in maintaining the integrity of
271 photosynthetic membranes during abiotic stress (Lippold et al., 2012). For only a small
272 fraction of genes, PS and CS showed similar cross-tissue memory response patterns (Figure
273 5A, Figure 2C). Among the different tissues, the most pronounced agreement was found for

274 young and mature leaves. The observed divergence between PS and CS was not due to the
275 fold change threshold ($\text{abs}(\log_2 \text{fold change}) > 1$); there were very few genes that satisfied the
276 significance threshold ($p.\text{adj} < 0.05$) but not the fold change threshold (Supplemental Figure 1).
277 Differences between PS and CS expression levels were consistent with the results of control-
278 based comparisons (Figure 5B).

279 The co-analysis of spatially separate tissues provided insights into the complexity of
280 coordinated whole-plant, long-term responses to periodically occurring stress. Strikingly, the
281 stress and recovery profiles of individual genes along the different trees were not conserved
282 across tissues (Figure 6). The expression patterns of the same gene correlated well across all
283 tissues for only 0.2% of the genes (Figure 6A). The largest number of self-correlated genes
284 was found between young and mature leaves, reflecting the functional similarity of these
285 compartments (Figure 6B). Furthermore, 995 genes were self-correlated between phloem and
286 xylem. Among these, functions in oxidation-reduction processes, carbohydrate and protein
287 metabolic processes as well as transmembrane transport and microtubule-based processes
288 were abundant. The genes with the strongest self-correlation across all tissues included a
289 large proportion of genes that exhibited a significant post-recovery memory pattern in PS
290 (Figure 6A, Supplemental Data Set 1). The top five of these genes were the transcription
291 factor genes *HOMEBOX7 (HB7) co-ortholog 1 (of 4)* (Potri.014G103000) and *HB7 co-*
292 *ortholog 3 (of 4)* (Potri.001G083700), as well as *GLUTAREDOXIN C1 co-ortholog 2 (of 2)*
293 (Potri.012G082800) and two clade A protein phosphatases of the 2C family (PP2Cs), the
294 *HIGHLY ABA-INDUCED1 (HAI1)* ortholog (Potri.009G037300) and Potri.001G092100. In
295 Arabidopsis, HB7 is transcriptionally induced by ABA and positively regulates PP2C gene
296 expression (Valdés et al., 2012).

297

298 **Transcription factors associated with stress-related memory**

299 Transcription factors (TFs) are key regulators at the top level of the molecular hierarchy.
300 Since several memory genes showed similar stress and post-recovery responses across all
301 tissues (Figure 6A), we were interested in whether common regulatory mechanisms exist
302 among different tissues that may play a role in stress-related memory. We used our gene
303 expression data from each tissue to infer regulatory relationships between known TFs
304 (Berardini et al., 2015; Jin et al., 2014) and these 17 self-correlated memory genes, resulting

305 in a gene regulatory network for each tissue (Figure 7, see Methods). Each of these tissue-
306 specific networks has one main connected component or forms a single connected
307 component, indicating that the self-correlated memory genes (Figure 7A, gray nodes) share
308 common top candidates of regulatory TFs (which were computationally inferred for each gene
309 by choosing the top five expression predictors; see Methods). The majority of candidate TFs
310 were tissue-specific (Figure 7A, white nodes), but a considerable fraction co-occurred across
311 two to four tissues. In particular, young and mature leaves shared ten candidate TFs. Edges
312 were also shared across tissues, meaning that a specific TF was found in several tissues
313 among the top five candidate regulators for a specific memory gene (Figure 7A, colored
314 edges; Figure 7B). A relationship between *HB7 co-ortholog 1 (of 4)* (Potri.014G103000) and
315 *HB7 co-ortholog 3 (of 4)* (Potri.001G083700) was predicted in all tissues except mature
316 leaves. In the co-expression analysis, both genes fell into the tissue-specific co-expression
317 modules of community C2, which was characterized by pronounced stress responses during
318 PS and CS (Figure 4, Supplemental Data Set 7). After recovery, a significant (20-fold) PS up-
319 regulation of *HB7 co-ortholog 3 (of 4)* gene expression was observed for both xylem and
320 mature leaves as well as a 200-fold PS up-regulation of *HB7 co-ortholog 1 (of 4)* for xylem. By
321 contrast, CS trees did not show significant changes in the expression of these genes relative
322 to control trees (Supplemental Data Set 1). The two *HB7*-related TF genes were also central
323 in the sense that together they covered all putative targets (non-TF memory genes) of their
324 subnetwork and their removal would disconnect the network into several parts (Figure 7B).
325 The *HB7* TFs are members of the homeodomain leucine zipper (HDZIP) family. In
326 *Arabidopsis*, *HB7* has been associated with drought stress responses as well as reduced cell
327 elongation in leaves and inflorescence stems (Hjellström et al., 2003; Söderman et al., 1996).
328 *HB7* has also been identified as a drought stress memory gene that showed a stronger up-
329 regulation at the third stress experience than after a single incidence (Ding et al., 2013).
330 Under non-stress conditions, *HB7* overexpression has been related to an increase in
331 chlorophyll content and photosynthesis rate (Re et al., 2014), which is consistent with our
332 physiological observations at the recovery phase.

333 The expression of the *HB7 co-ortholog 1 (of 4)* (Potri.014G103000) gene itself is putatively
334 related to the expression of the TF gene Potri.006G138900, which was found to be a co-
335 predictor with Potri.001G083700 for several putative target genes, and Potri.002G125400
336 (Figure 7B). Potri.002G125400 is annotated as *ABSCISIC ACID RESPONSIVE ELEMENTS-*

337 *BINDING FACTOR2 (ABF2) co-ortholog 1 (of 2)*. Arabidopsis ABF2 is known to enhance
338 drought tolerance (Nakashima et al., 2014). Potri.006G138900 is a member of the ethylene
339 response factor/APETALA2 (ERF/AP2) TF family. The closest Arabidopsis ortholog in its
340 evolutionary family, PTHR31985:SF77 (Mi et al., 2017), is AT5G21960, which belongs to the
341 DREB subfamily A-5, with established functions in drought stress response (Singh and Laxmi,
342 2015). In poplar, the Potri.006G138900 gene has been reported to be induced by four
343 different types of osmotic stresses (Yao et al., 2017). In our data, significant up-regulation of
344 this gene was only observed for PS and not for CS. In Arabidopsis, *RELATED TO AP21*
345 (*RAP2.1*), a prominent member of the DREB gene subfamily A-5, is also more strongly
346 induced after the repeated application of dehydration stress (Ding et al., 2013). *RAP2.1* is a
347 negative regulator of *RD/COR (RESPONSIVE TO DESICCATION/ COLD-REGULATED)*
348 genes (Dong and Liu, 2010). Poplar *RAP2.1* Potri.014G025200 and the other poplar DREB
349 TF that most closely matches Arabidopsis *RAP2.1* were significantly up-regulated in xylem
350 during both PS and CS. Consistently, the *COR413* gene Potri.007G033801 was significantly
351 down-regulated under these conditions.

352 A relationship between two (TEOSINTE BRANCHED1, CYCLODEA, PROLIFERATING CELL
353 FACTORS (TCP) family TFs was detected in young and mature leaves (Figure 7B,
354 Supplemental Data Set 8). Both TFs, Potri.013G119400 and Potri.019G091300, are most
355 similar to the Arabidopsis TF TCP4. The expression of Potri.013G119400 was significantly
356 down-regulated after recovery from PS in both young and mature leaves compared with the
357 untreated controls. During PS and CS, both TFs were transcriptionally down-regulated in
358 young and mature leaves (Supplemental Data Set 1). In the remaining tissues, the expression
359 patterns of the two TFs diverged from each other. For the developing xylem,
360 Potri.013G119400 was down-regulated but Potri.019G091300 was up-regulated. The putative
361 leaf target, Potri.010G230366, does not have a known function, but its expression was also
362 strongly up-regulated in developing xylem under both PS and CS, and after recovery from PS,
363 up-regulation was more than 50-fold. Potri.013G119400 expression was also down-regulated
364 in phloem and roots, whereas there was no change in expression for Potri.019G091300.
365 TCP4 has been associated with cell elongation in hypocotyls and leaf morphogenesis (Challa
366 et al., 2016). The differential regulation of these genes across tissues during stress and
367 recovery in gray poplar may reflect different cell growth dynamics. While water deficiency
368 generally suppresses growth in aboveground poplar tissues, xylem structure and secondary

369 cell wall formation play a central role in avoiding drought damage and are highly regulated
370 (Paul et al., 2018; Sun et al., 2017).

371

372 **Common and tissue-specific processes involved in stress-related memory**

373 To further elucidate and compare stress-related memory processes that take place in
374 individual poplar tissues, we investigated the regulatory networks in mature leaves and
375 developing xylem (Figure 8). These were the two tissues where the HB7 TFs, the top
376 correlated genes within and across tissues (Figure 7B, Figure 6A), showed the strongest
377 post-recovery memory response (Supplemental Data Set 1). For each tissue network, we
378 specifically focused on TFs that were computationally associated with more than one putative
379 target as predictors of gene expression (Figure 8A). Among the targets that were included in
380 the core networks of both mature leaves and developing xylem, we found two *PP2Cs* (the
381 *HAI1* ortholog (Potri.009G037300) and an *HAI3*-related *PP2C*, Potri.001G092100), the two
382 *LATE EMBRYOGENESIS ABUNDANT PROTEIN4-5 (LEA 4-5)* co-orthologs and a gene of
383 unknown function with almost 100-fold up-regulation in PS and more than 150-fold up-
384 regulation after PS recovery in mature leaves (Potri.004G044300), whose closest *Arabidopsis*
385 match has been reported to be induced by ABA in guard cells (Leonhardt et al., 2004). The
386 two *PP2Cs* and the *LEA4-5* homologs were also up-regulated during PS and after PS
387 recovery in mature leaves (Figure 8A). *LEA4-5* protein levels strongly increase in poplar
388 under drought stress conditions for osmoprotection (Abraham et al., 2018). In *Arabidopsis*,
389 *LEA4-5* transcript and protein levels showed the largest response to ABA and salt stress
390 within the *LEA4* group (Olvera-Carrillo et al., 2010).

391 *PP2Cs* are negative regulators of ABA signaling and hamper stomatal closure, as
392 demonstrated by the protein interactions of the *PP2C* HYPERSENSITIVE TO ABA1 (*HAB1*)
393 in *Populus euphratica* and the *PP2C* ABA-INSENSITIVE1 (*ABI1*) in *Populus trichocarpa*, as
394 well as the analysis of transgenic *Arabidopsis* plants overexpressing these genes (Chen et
395 al., 2015; Yu et al., 2016). In *Arabidopsis*, the *PP2C* *HAI1* (SAG113; AT5G59220) prevents
396 stomatal closure during leaf senescence, and its promoter is directly targeted by a NAC TF
397 (*NAC029*, AtNAP; AT1G69490) (Zhang and Gan, 2012). In the mature leaf regulatory network
398 inferred from our data, the expression of the *HAI1* ortholog (Potri.009G037300) was not only
399 associated with the expression of the *HB7*-related TF genes (Potri.014G103000,

400 Potri.001G083700) but also with the expression of the NAC TF gene Potri.011G123300 and
401 the MYB family TF genes Potri.010G193000 and Potri.003G100100, which belong to different
402 ortholog groups (Figure 8A). The association between the latter three genes and the *HAI1*
403 ortholog was not detected in developing xylem. In fact, the Pearson correlation coefficients in
404 developing xylem were 0.61, 0.30 and 0.26, respectively, in contrast to the highly significant
405 values in mature leaves (0.94, 0.91 and 0.93). The gene Potri.011G123300 belongs to the
406 NAC TF family due to its NAM (no apical meristem) domain; it is a member of the NAC019-
407 related subfamily of orthologs, PTHR31719:SF82 (Mi et al., 2017). NAC TFs, particularly the
408 three Arabidopsis members of that subfamily, NAC019, NAC055 and NAC072, are of central
409 importance in drought signal transduction via the ABA-dependent pathway (Singh and Laxmi,
410 2015; Tran et al., 2004). Gene expression of the MYB TF Potri.010G193000 is negatively
411 correlated with the wood saccharification potential in poplar, which decreases under drought
412 conditions (Wildhagen et al., 2018). Consistent with this observation, our expression data
413 showed that Potri.010G193000 was up-regulated under stress. The same pattern was
414 observed for mature leaves and in the case of PS, even persisted after recovery.
415 Furthermore, Potri.010G193000 is in general co-expressed with Potri.007G085700, the TF
416 gene *TGACG SEQUENCE-SPECIFIC BINDING PROTEIN1 (TGA1)* (Wildhagen et al., 2018).
417 Interestingly, several Arabidopsis orthologs of inferred regulators of HAI1 in mature poplar
418 leaves were connected via experimental and literature-curated protein-protein interaction data
419 (Arabidopsis Interactome Mapping Consortium, 2011; Berardini et al., 2015; Yazaki et al.,
420 2016), including TGA1 (Figure 8B). The *TCP4* orthologs discussed above (Potri.019G091300,
421 Potri.013G119400) were strongly transcriptionally anti-correlated with the *HB7* co-ortholog
422 Potri.001G083700, which was found to be a central predictor for the two *PP2Cs* and both
423 *LEA4-5* orthologs in mature leaves.

424 In developing xylem, the *HB7* co-ortholog Potri.001G083700 was also associated with these
425 *PP2Cs* and *LEA4-5* orthologs, which have known physiological functions related to drought
426 responses. In both tissues, Potri.001G083700 continued to be up-regulated after PS
427 recovery. In addition, the core networks of xylem and mature leaves shared the putative
428 target *GLUTAREDOXIN C1 (GRXC1) co-ortholog 2 (of 2)* (Potri.012G082800), showing post-
429 recovery PS up-regulation in both tissues. With respect to abiotic stress, GRXC1 plays roles
430 in signaling and oxidative stress tolerance (Li, 2014). Another shared putative target was
431 Potri.002G117800, one of two *NADH DEHYDROGENASE (UBIQUINONE) FE-S PROTEIN4*

432 (*NDUFS4*) genes involved in the mitochondrial electron transfer chain that have been
433 associated with thermotolerance in Arabidopsis (Kim et al., 2012). With respect to additional
434 TFs, the xylem network showed several differences from the network from mature leaves
435 (Figure 8A). The ERF/AP2 DREB TF Potri.006G138900 (also see previous section) was a
436 large hub, in addition to the HB7 TF Potri.001G083700, which formed a central hub in both
437 tissues. The BHLH18-related TF Potri.009G081400 (BASIC HELIX-LOOP-HELIX18) was
438 unique to the xylem network, associated with *GRX1*, *LEA4-5* and both *PP2Cs*, and still
439 significantly up-regulated after PS recovery. A xylem-specific, putative regulator of both HB7
440 TFs was the BHLH TF Potri.014G111400, one of three *PHYTOCHROME-INTERACTING*
441 *FACTOR3 (PIF3)* genes. Arabidopsis PIF3 promotes hypocotyl elongation (Soy et al., 2012;
442 Zhong et al., 2012). In summary, our data suggest that common TFs such as the HB7
443 homologs, particularly the central hub gene Potri.001G083700, work together with tissue-
444 specific TFs to coordinate stress and post-recovery processes in different tissues.

445

446 **DISCUSSION**

447 Although drought stress is one of the major threats to plant growth, it is well-known that plants
448 that have endured stress can show better photosynthetic performance than non-exposed
449 plants under both subsequent stress (Wang et al., 2014) and well-watered conditions
450 (Hagedorn et al., 2016), which may even lead to over-compensating plant growth (Xu et al.,
451 2010). We investigated gray poplar trees that had experienced three weeks of drought-heat
452 stress. After one week of recovery, we observed not only a complete reconstitution of
453 transpiration and photosynthetic capacity along with a relaxation of water potentials but also
454 an increased rate of carbon gain compared to non-stressed controls, for both a periodic and a
455 chronic stress scenario. Transcriptomic analyses across five different organs and tissues
456 revealed cellular processes occurring in response to combined drought and heat stress and
457 after recovery. Post-recovery expression patterns showed significant differences from non-
458 treated poplar trees and also between the two stress scenarios, although the PS and CS
459 responses had been highly similar at the end of the stress phase. This observation
460 substantiates the hypothesis that stress exposure influences the physiological state of a plant
461 even after recovery and that this long-term response varies according to the frequency or
462 duration of the stress intervals. This memory phenomenon in trees already occurs a few days

463 after the stress has ceased, which hints at powerful molecular mechanisms that could
464 potentially also make a difference in plant fitness across multiple successive years. Such a
465 life-cycle investigation was outside the scope of the current study. However, the results show
466 that such a long-term investigation might be highly valuable when carefully designed.

467 Similar expression patterns in response to stress and after recovery were found throughout
468 the tree. However, they were implemented by distinct genes in each tissue. Only a small
469 number of genes showed a consistent response profile across all tissues. Apart from genes
470 encoding signaling components and enzymes such as PP2Cs and GRXC1 or proteins with
471 structural function like the LEA4-5 hydrophilins (Battaglia et al., 2008), this set of genes with
472 putatively ubiquitous function contained several TFs, most prominently two HB7 homologs
473 that also showed a PS-related post-recovery up-regulation. HB7 contains a homeodomain
474 and a leucine zipper motif. This protein architecture indicates that the TF forms dimers (Ariel
475 et al., 2007). TF homo- or heterodimerization as well as multimerization allow for a high
476 degree of regulatory fine-tuning of gene expression. We therefore speculate that TF
477 complexes might play a role in shaping stress and post-recovery regulation of gene
478 expression in the tissue-specific context (Figure 8B). Protein-protein interaction data from the
479 model system Arabidopsis suggest that HB7 and some TFs from the NAC019 and MYB TF
480 families with leaf-specific responses in poplar (best Arabidopsis matches AT4G27410 and
481 AT5G05790, respectively) may all associate with TGA1 and a set of ZHD (zinc-finger
482 homeodomain) TFs, which were expressed in all poplar tissues according to our dataset.
483 Another putative interactor of TGA1, the only HEAT STRESS TRANSCRIPTION FACTOR C-
484 1 (HSFC1) TF in poplar (Potri.T137400), was predicted to be a regulator of the *HB7* co-
485 ortholog Potri.001G083700 and the two *PP2Cs* in phloem-bark (Supplemental Data Set 8).
486 Members of the ZHD TF family form heterodimers that play a crucial role in floral
487 development (Tan and Irish, 2006) as well as ABA responses (Wang et al., 2011) in
488 Arabidopsis. Co-expression of the NAC019 family gene AT4G27410 and ZHD11 strongly
489 induces the expression of *EARLY RESPONSIVE TO DEHYDRATION STRESS1*, which is
490 up-regulated by drought through the ABA-independent pathway (Tran et al., 2007).

491 The combined action of several TFs might regulate the expression of target genes. The up-
492 regulation of *PP2Cs* in mature poplar leaves observed in the current study is consistent with
493 the positive regulatory role of HB7 in *PP2C* expression reported for Arabidopsis (Valdés et al.,
494 2012). Furthermore, NAC TFs regulate the *PP2C HAI1* (Zhang and Gan, 2012) and other

495 drought tolerance genes (Singh and Laxmi, 2015; Tran et al., 2004). PP2Cs inactivate type-2
496 SNF1-related protein kinases (SnRK2s), which are positive regulators of ABA signaling,
497 stomatal closure and chlorophyll degradation (Fujii et al., 2011; Gao et al., 2016; Kulik et al.,
498 2011; Nakashima et al., 2009; Valdés et al., 2012). Consistently, HB7 overexpression leads to
499 an increased chlorophyll content and a higher rate of photosynthesis (Re et al., 2014).
500 Moreover, various PP2Cs interact with the photosynthetic machinery (Fuchs et al., 2013;
501 Samol et al., 2012), and photosynthesis genes are up-regulated in Arabidopsis *snrk2* triple
502 mutants (Nakashima et al., 2009), pointing to a relationship between PP2Cs and
503 photosynthesis. Translating these findings to poplar, the model would explain the improved
504 photosynthesis detected in recovered poplar trees after periodic stress (Figure 8C).
505 Chlorophyll content estimates did not show differences from the controls (Vanzo et al., 2015)
506 but were done non-invasively, in contrast to the Arabidopsis studies (Gao et al., 2016; Re et
507 al., 2014). The increase in ABA levels during drought stress inhibits the enzyme activity of
508 clade A PP2Cs like HAI1 and HAI3 via interacting ABA receptors (Dupeux et al., 2011;
509 Tischer et al., 2017). Due to this mechanism, leaf stomata can close during drought to prevent
510 excessive water loss (Figure 8C). For poplar, stress-induced stomatal closure was confirmed
511 by our measurements of transpiration and stomatal conductance. Protein-protein interactions
512 of PP2Cs with a SnRK2 kinase and pyrabactin resistance-like ABA receptors and their effect
513 on leaf stomatal closure in transgenic plants have been shown for several poplar species
514 (Chen et al., 2015; Yu et al., 2016), providing evidence for the potential roles of PP2Cs in
515 poplar leaves during and after stress. Apart from that, PP2Cs may also be involved in
516 chromatin remodeling and the establishment of an epigenetic memory after stress (Asensi-
517 Fabado et al., 2017).

518 The system-wide rearrangement of gene expression after stress recovery might also
519 contribute to the improved tolerance against future stresses described previously (Crisp et al.,
520 2016; Hilker et al., 2016; Wang et al., 2014). In Arabidopsis, *HB7* and *LEA4-5*, prominent
521 memory-related genes based on our study, are more strongly induced during repeated
522 dehydration stress challenges than during the first stress challenge (Ding et al., 2013).
523 Complementing such studies on recurrence-dependent changes in stress responses, our data
524 provide a comprehensive view of stress-related molecular memory under non-stress, post-
525 recovery conditions. The increased base levels of *HB7* and *LEA4-5* gene expression after
526 stress recovery could potentially explain their higher expression levels during subsequent

527 stress challenges. Consistent with such a model, the periodic stress response was greater
528 than the chronic stress response in leaves, and the increase in post-recovery base level was
529 only significant for periodic stress and not for chronic stress, suggesting a gradual base level
530 increase along with several stress experiences. The same trend was observed in the
531 photosynthesis data. A better understanding of the molecular changes, their timing, and their
532 impact on the performance of plants is instrumental for providing guidelines for resource-
533 efficient agroforestry water management and in the breeding of crop and tree cultivars that
534 are genetically equipped for climate change scenarios. The present evaluation indicates that
535 transcription factors function as central switches of molecular memory and may be important
536 mediators of plant fitness during the persistent adaptation to recurrent abiotic stress. The
537 biological hypotheses generated by our comprehensive data acquisition and integration pave
538 the way for detailed mechanistic studies that will provide deeper insights into memory-related
539 molecular processes in plants.

540

541 **METHODS**

542 **Plant material**

543 The experiments were performed with wild-type gray poplar (*Populus x canescens* [INRA
544 clone 7171-B4]; syn. *Populus tremula x Populus alba*) plants. Plantlets were amplified by
545 micro-propagation under sterile conditions (Leple et al., 1992) and raised for five weeks in
546 2.2-L pots on a sandy soil (1:1 [v/v] silica sand and Fruhstorfer Einheitserde, initially mixed
547 with slow-release fertilizers: Triabon [Compo] and Osmocote [Scotts Miracle-Gro], 1:1, 10 g L⁻¹
548 soil; fertilized every two weeks with 0.1% [w/v] Hakaphos Grün [Compo]) in the greenhouse
549 (16/8 h photoperiodicity with supplemental lighting (high-pressure sodium vapor lamp, Philips
550 Son-T agro, Hamburg, Germany), 200-240 $\mu\text{mol photons m}^{-2} \text{ s}^{-1}$ at the canopy level,
551 photosynthetically active radiation [PAR]; day/ night temperature 22 °C/ 18 °C; and an
552 ambient mean CO₂ concentration of 380 $\mu\text{L L}^{-1}$). To simulate specific climate scenarios, the
553 plants were moved to phytotron chambers (see below). Within each chamber, 12 plants were
554 cultivated together in a gas-tight sub-chamber made of acrylic glass ($\sim 1 \text{ m}^3$), which enabled
555 online analysis of canopy gas exchange (Vanzo et al., 2015).

556

557 **Simulated climate conditions and harvesting schedule**

558 The future climate scenarios simulated in our experiments comprised elevated CO₂ (EC) and
559 two abiotic stress scenarios under elevated CO₂, periodic drought-heat stress (PS) and
560 chronic drought-heat stress (CS). Before starting the abiotic stress scenarios, plants were
561 cultivated for 25 days in the phytotron chambers under control conditions (daily maximum air
562 temperature of 27°C, 50% relative air humidity) with either ambient (380 μL L⁻¹) or elevated
563 (500 μL L⁻¹) CO₂. The CO₂ concentrations in all scenarios followed natural occurring diurnal
564 variations. The elevated CO₂ environment in the EC, PS and CS scenarios was created by
565 injection of pure CO₂ (+ 120 μL L⁻¹) into the air stream of the ambient CO₂. At the top of the
566 phytotron chambers, a combination of four lamp types (metal halide lamps: Osram Powerstar
567 HQI- TS 400W/D [Osram, München, Germany]), quartz halogen lamps: Osram Haloline
568 500W, blue fluorescent tubes: Philips TL-D 36W/BLUE, and UV-B fluorescent tubes: Philips
569 TL 40W/12) was used to obtain a natural balance of simulated global radiation throughout the
570 UV to infrared spectrum. The lamp types were arranged in several groups to get the natural
571 diurnal variations of solar irradiance by switching appropriate groups of lamps on and off. The
572 short-wave cut-off in the UV-B range of the spectrum was achieved by selected soda-lime
573 and acrylic glass filters. A detailed description of the sun simulator facility is given by Thiel et
574 al. (1996). The PAR at canopy level was 750-800 μmol photons m⁻² s⁻¹.

575 For chronic stress treatment, irrigation was gradually reduced for 22 days, down to 70%
576 reduction compared with the controls. The periodic stress treatment included three cycles of
577 reduced irrigation (50%, 60% and 70% reduction compared to controls), each one lasting for
578 six days; between the cycles, there were recovery periods lasting two days. In both stress
579 scenarios, the daily maximum air temperature was set to 33°C during periods with reduced
580 irrigation. Non-invasive gas exchange measurements were made continuously; destructive
581 harvests of six plants per chamber were performed at the end of the stress phase and after
582 one week of recovery (Vanzo et al., 2015). Mid-day shoot water potentials (ψ_{md}) were
583 determined at each sampling date (n=6 plants per treatment, mean \pm se) using a Scholander
584 pressure chamber (Scholander et al., 1965). In chronically and periodically stress-treated
585 plants, ψ_{md} was more negative (-1.52 \pm 0.10 and -1.27 \pm 0.05 MPa, respectively) compared to a
586 ψ_{md} of -0.97 \pm 0.04 MPa in AC and of -0.97 \pm 0.07 MPa in EC shoots. At recovery, ψ_{md} went
587 back to -0.72 \pm 0.10 and -0.93 \pm 0.07 MPa in PS and CS, respectively, reaching comparable
588 values to the untreated controls in AC (-0.77 \pm 0.07 MPa) and EC (-0.90 \pm 0.06 MPa).

589

590 **Gas exchange measurements**

591 Leaf-level gas exchange measurements were performed using two GFS-3000 instruments
592 (Walz, Germany) with an 8 cm² clip-on-type cuvette on attached leaves (no. 9 from the apex)
593 of four biological replicates under standard conditions (30°C, 1000 μmol photons m⁻² s⁻¹, and
594 air humidity of 10,000 μL L⁻¹). The cuvette was flushed with synthetic air with the CO₂
595 concentration of the respective growth condition. For each climate chamber, CO₂ and water
596 concentrations in the ambient air were measured every 20 min with two infrared gas
597 analyzers (Rosemount 100/4P, Walz, Germany) from the outlet of the gas-tight sub-chamber
598 containing the plants. Inlet air was also measured every 20 min. The whole plant (canopy) net
599 CO₂ assimilation and evapotranspiration rates (A and E , respectively) were calculated based
600 on the difference between the outlet and inlet concentrations of each sub-chamber (see
601 Appendix 2, von Caemmerer and Farquhar, 1981): $A = \frac{u_e}{s} \left(\frac{1-w_e}{1-w_0} \right) (c_e - c_0) - E \cdot c_e$ and $E =$
602 $\frac{u_e}{s} \left(\frac{w_0-w_e}{1-w_0} \right)$, where w_e and w_0 are the mole fractions of water vapor and c_e and c_0 the mole
603 fractions of CO₂ in the incoming and outgoing airstreams, respectively, u_e is the molar flow of
604 air entering the chamber, and s is the canopy leaf area, which was estimated every day (Jud
605 et al., 2016; Vanzo et al., 2015).

606

607 **Organ and tissue sampling**

608 Plants were harvested at noon on the last day of stress treatment and seven days later at the
609 end of the recovery period. Leaves (young leaves n. 4-6, mature leaves n. 9-12 counting from
610 the apex, respectively) were immediately frozen in liquid N₂. A stem segment was cut 10 cm
611 above the stem base and immediately frozen in liquid N₂. The roots were washed three times
612 in water, carefully dabbed with filter paper, and frozen in liquid N₂. All material was stored at -
613 80 °C until homogenization. Homogenization of plant materials was performed under liquid N₂
614 with a mortar and pestle. The bark containing the phloem tissue was removed from the stem
615 section with a scalpel. Young developing xylem tissue was obtained by scraping off the first
616 1–2 mm of the hardwood section. The homogenized mature leaf material was used for both
617 biochemical analysis and RNA extraction, and all other materials were used only for RNA

618 extraction. Although leaf and root samples were mixtures of several tissues, the different plant
619 materials are referred to as tissues throughout this work.

620

621 **Biochemical measurements of the antioxidative system**

622 Enzyme activities and molecular antioxidant levels from four biological replicates were
623 determined as previously described (AbdElgawad et al., 2016). Molecular antioxidants were
624 quantified by HPLC after extracting frozen plant materials in hexane (tocopherols) or ice-cold
625 meta-phosphoric acid (ascorbate, glutathione). The enzyme activities of superoxide
626 dismutase, peroxidase, catalase, ascorbate peroxidase, glutathione peroxidase, glutathione
627 reductase, dehydroascorbate reductase, and monodehydroascorbate reductase were
628 determined using a micro-plate reader after extracting frozen plant materials in potassium
629 phosphate buffer supplemented with protease inhibitors.

630

631 **RNA-seq analysis**

632 RNA extraction was performed as described by Bi et al. (Bi et al., 2015). Total RNA was
633 extracted from 50 mg frozen tissue using an Aurum Total RNA Mini kit (Bio-Rad, Germany)
634 following the manufacturer's instructions. The RNA concentration was quantified using a
635 NanoDrop 1000 spectrophotometer (NanoDrop, Peqlab GmbH, Erlangen, Germany). The
636 260/230 and 260/280 ratios were in the range of 1.90 to 2.67 (mean 2.21) and 1.94 to 2.45
637 (mean 2.12), respectively. RNA integrity was confirmed using an Agilent Bioanalyzer 2100
638 (Agilent Technologies, USA). For each specific combination of environmental condition, time
639 point and tissue, RNA samples from three biological replicates were analyzed by Illumina
640 sequencing (100 bp single reads, HiSeq 2500, Illumina, Inc., San Diego, CA, USA) of mRNA
641 libraries (NEBNext Ultra directional RNA library prep Kit Illumina, New England Biolabs, Inc.,
642 Ipswich, MA, USA), yielding RNA-seq reads for 120 samples in total. The biological replicates
643 are samples from different individual trees grown under the same condition and harvested at
644 the same time. For each tree, samples from all five tissues were sequenced, except for two
645 cases where RNA extraction from the initial sample failed (260/230 ratio 0.42 and 1.4,
646 respectively) and samples from additional trees had to be taken as replacement: AC recovery
647 root sample replicate 1 and PS stress xylem sample replicate 3 (Supplemental Data Set 9).

648 RNA-seq reads were aligned against the repeat-masked version of the *Populus trichocarpa*
649 reference genome (assembly version v3.0) (Tuskan et al., 2006) using TopHat2 (Kim et al.,
650 2013). To account for the evolutionary distance between gray poplar and the reference
651 genome, different alignment stringency levels were tested. For that purpose, three different
652 sequencing libraries were randomly selected and RNA-seq reads mapped against the
653 reference genome, allowing two to six mapping errors per read (Supplemental Figure 2).
654 Approximately 70% of the RNA-seq reads were aligned when allowing a maximum of five
655 errors in the read alignments, which is relatively similar to RNA-seq analysis in other plants
656 (International Barley Genome Sequencing Consortium et al., 2012). Due to the relatively
657 constant proportion of uniquely mapped reads for the considered error levels (Supplemental
658 Figure 2B), we continued the analysis with the maximum threshold of five errors
659 (Supplemental Figure 3).

660 Based on the read alignments and the *P. trichocarpa* annotation version v3.1 at the
661 Phytozome platform (Goodstein et al., 2012; Tuskan et al., 2006), TPM gene expression
662 levels were calculated using StringTie version 1.3.4 (Pertea et al., 2015). The biological
663 replicates showed high Pearson correlation coefficients (computed by the cor function in R
664 version 3.5.0 (R Core Team, 2018)) except for one single case (Supplemental Figure 4),
665 which was excluded from further analysis. Differentially expressed genes between PS or CS
666 and EC groups were identified using the R package DESeq2 version 1.20.0 (Love et al.,
667 2014) using the script provided at <http://ccb.jhu.edu/software/stringtie/dl/prepDE.py>. Gene
668 annotation including functional description, InParanoid orthology and Gene Ontology (GO)
669 terms were retrieved from the *Populus trichocarpa* reference annotation version v3.1 at the
670 Phytozome platform (Goodstein et al., 2012; Tuskan et al., 2006). GO enrichment analysis for
671 categories with at least 50 genes was performed in R version 3.5.0 (R Core Team, 2018)
672 using fisher.test and multiple testing correction by p.adjust using the false discovery rate
673 (FDR) method.

674

675 **Co-expression network analysis**

676 The co-expression network analysis focused on the environmental conditions with elevated
677 CO₂ levels, omitting the AC (ambient CO₂) condition. For each tissue, log₂(TPM+1)-
678 transformed gene expression levels were averaged for each condition and time point and

679 genes were filtered for a minimum coefficient of variation of 0.3 (Supplemental Figure 5).
680 Individual co-expression modules for each tissue were determined using the R packages
681 WGCNA version 1.64-1, flashClust version 1.01-2 and dynamicTreeCut version 1.63-1
682 (Langfelder and Horvath, 2008, 2012; Langfelder et al., 2008). The parameters were set to
683 "hybrid signed" network, "average" agglomeration, split sensitivity 1 and a minimum cluster
684 size of 50. The module eigengenes (Langfelder and Horvath, 2007), characteristic expression
685 profiles of modules, were clustered across all tissues into communities according to their
686 correlation. This step was performed using flashClust and dynamicTreeCut ("average"
687 agglomeration, deep split set to true and a minimum cluster size of 2). Communities that
688 contained modules from all five tissues were visualized with the tkplot and plot functions in the
689 R package igraph version 1.2.2 (Csardi and Nepusz, 2006). The corresponding heatmaps
690 were plotted using the R packages pheatmap version 1.0.10, gridExtra version 2.3 and
691 ggplot2 version 2.2.1 (Auguie, 2017; Kolde, 2018; Wickham, 2009).

692

693 **Between-tissue correlations and gene regulatory network analysis**

694 To investigate tissue-specific regulation of universally responding genes, we first determined
695 individual genes that behaved similarly in all the tissues and then predicted their regulation by
696 transcription factors (TFs) using the RNA-seq data. In the first step, gene-gene correlations
697 across individual trees from all treatment groups were computed using the cor function in R
698 version 3.5.0 on the $\log_2(\text{TPM}+1)$ -transformed gene expression data (R Core Team, 2018). In
699 particular, correlation values of the same gene across all pairs of tissues were recorded and
700 the 17 genes with a median greater than 0.8 and significant post-recovery difference to
701 controls in at least one tissue ($\text{abs}(\log_2 \text{ fold change}) > 1$ and $p.\text{adj} < 0.05$ according to the
702 DESeq2 analysis) were selected as query genes for further analysis. Since observations for
703 these genes were quite complete (less than 20 values with expression level zero in the whole
704 dataset with 119 samples), we focused the regulatory network analysis on genes with at most
705 20 zero values. TF family annotation for *Populus trichocarpa* and *Arabidopsis thaliana* was
706 downloaded from PlantTFDB (Jin et al., 2014) on 03.09.2018. Poplar genes were included as
707 candidate TFs in the analysis if they themselves as well as their best Arabidopsis match
708 according to the Phytozome annotation v3.1 (Goodstein et al., 2012; Tuskan et al., 2006)
709 were both classified as TFs, resulting in 1346 candidates. For each query gene, the top

710 regulatory candidates were determined from the gene expression data of each tissue
711 separately using the R package GENIE3 version 1.2.1 (Aibar et al., 2017; Huynh-Thu et al.,
712 2010). Networks were drawn with the R package igraph version 1.2.2 (Csardi and Nepusz,
713 2006). For visualization purposes, the top five candidates are shown for each query gene.

714

715 **Protein-protein interaction analysis**

716 Experimental and literature-curated protein-protein interaction data for *Arabidopsis thaliana*
717 were obtained from datasets of interactome publications and from the TairProteinInteraction
718 file (time stamp: 2011-08-23) at The Arabidopsis Information Resource (Arabidopsis
719 Interactome Mapping Consortium., 2011; Berardini et al., 2015; Yazaki et al., 2016) and
720 compiled into a single network. The network was visualized with Graphviz version 2.36
721 (Gansner and North, 2000). Due to the prominent transcriptional stress-related memory
722 response observed for the HB7 TF Potri.001G083700 and its predicted target, the HAI1
723 ortholog Potri.009G037300, combined with the known physiological role of HAI1 in
724 *Arabidopsis thaliana* leaves and the dimerization motif of HB7, we investigated the
725 interactomes of Arabidopsis orthologs given in Phytozome (Goodstein et al., 2012; Tuskan et
726 al., 2006) for all TFs that were predicted to regulate Potri.009G037300 in mature leaves and
727 showed a significant differential expression in PS vs. EC after recovery. The subnetwork
728 connecting AT2G46680 (HB7) and AT4G27410 (closest match from the NAC019 orthology
729 group) was evident from visual inspection of the network, and the connection to the MYB TF
730 AT5G05790 was found computationally by neighborhood intersection. All three TFs did not
731 have any other interactions than the ones shown in the subnetwork (Figure 8B).

732

733 **Further statistical analysis**

734 Treatment group comparisons for the gas exchange and antioxidant data were performed
735 using the R package dunn.test with the FDR method "bh" as a post-hoc Dunn's test after
736 application of the Kruskal-Wallis test using kruskal.test in R version 3.5.0 (R Core Team,
737 2018). Dimension reduction for data visualization was also done in R. To show common
738 variation between the gas exchange data (eight parameters) and the $\log_2(\text{TPM}+1)$ -
739 transformed gene expression data in mature leaves, we selected the 100 most varying genes

740 and applied regularized canonical correlation analysis using the rcc function from the
741 mixOmics package version 6.3.2 (Gonzalez et al., 2011; Le Cao et al., 2009) and an
742 analytical estimate of the regularization parameter (Schäfer and Strimmer, 2005). Principal
743 component analysis of the whole gene expression dataset was performed with the prcomp
744 function in R version 3.5.0 (R Core Team, 2018). Ellipses for 75% confidence levels were
745 constructed from the expression data using the dataEllipse function of the R package car
746 version 3.0-2 (Fox and Weisberg, 2011). Venn diagrams for differentially expressed genes
747 ($\text{abs}(\log_2 \text{ fold change}) > 1$ and $\text{p.adj} < 0.05$ according to the DESeq2 analysis) were created
748 with the R package venn version 1.7 (Dusa, 2018), and the gene-wise expression heatmap
749 was generated with the heatmap.2 function of the gplots R package version 3.0.1 (Warnes et
750 al., 2016).

751

752 **Accession numbers**

753 The RNA-seq data have been deposited in the ArrayExpress database at EMBL-EBI
754 (<https://www.ebi.ac.uk/arrayexpress/experiments/E-MTAB-6121>). R scripts for the data
755 analysis are available at <https://github.com/georgii-helmholtz/samm>.

756

757 **Supplemental Data**

758 **Supplemental Figure 1.** Volcano plots for differential expression analysis of stress-treated
759 trees relative to control trees in tissues harvested after recovery.

760 **Supplemental Figure 2.** Parameter selection for the alignment of RNA-seq reads.

761 **Supplemental Figure 3.** RNA-seq read mapping statistics.

762 **Supplemental Figure 4.** Gene expression correlation between biological replicates.

763 **Supplemental Figure 5.** Selection of genes used for co-expression network analysis.

764 **Supplemental Data Set 1.** Annotation and differential expression of stress (PS, CS) vs.
765 control (EC) samples for all genes found in the RNA-seq analysis.

766 **Supplemental Data Set 2.** GO enrichment analysis of stress phase up-regulated genes (log₂
767 fold change > 1, p.adj < 0.05) shared between PS and CS or specific to one of the stress
768 scenarios.

769 **Supplemental Data Set 3.** GO enrichment analysis of stress phase downregulated genes.

770 **Supplemental Data Set 4.** GO enrichment analysis of recovery phase upregulated genes.

771 **Supplemental Data Set 5.** GO enrichment analysis of recovery phase downregulated genes.

772 **Supplemental Data Set 6.** Biochemical parameters of the anti-oxidative system (anti-oxidant
773 levels and enzyme activities).

774 **Supplemental Data Set 7.** Co-expression modules identified from phase- and condition-
775 dependent gene expression profiles for each tissue.

776 **Supplemental Data Set 8.** Tissue-specific gene regulatory networks for query genes that
777 responded similarly across all tissues and showed a significant stress-related memory effect.

778 **Supplemental Data Set 9.** Tree origin and RNA-seq alignment statistics of tissue samples.

779

780 **ACKNOWLEDGMENTS**

781 The work was financially supported by the European Science Foundation (ESF) Eurocores
782 programme 'EuroVOL' within the joint research project 'MOMEVIP', the European Plant
783 Phenotyping Network (EPPN) funded by the EU FP7 Research Infrastructures Programme
784 [no. 284443], the German Ministry of Education and Research projects 'PROBIOPA' [no.
785 0315412] and German Plant Phenotyping Network (DPPN) [no. 031A053C], the Belgian Fund
786 for Scientific Research [no. GA13511N] and by the Austrian Science Funds [no. I655-B16].
787 The authors thank Pascal Falter-Braun, Daniel Lang and Georg Haberer for helpful
788 comments.

789 **AUTHOR CONTRIBUTIONS**

790 J.-P.S., K.F.X.M., K.P., H.A. and A.H. designed the research. E.V., M.A.D., W.J. and R.R.
791 performed the experiments. E.G., K.K., M.P., K.B., H.AE. and M.S. analyzed the data. E.G.

792 wrote the paper with contributions of J.-P.S., K.F.X.M., K.K., K.P., A.R.S. and M.S.; all
793 authors checked and revised the manuscript.

794

795 REFERENCES

796

797 AbdElgawad, H., Zinta, G., Hegab, M.M., Pandey, R., Asard, H., and Abuelsoud, W. (2016).
798 High salinity induces different oxidative stress and antioxidant responses in maize seedlings
799 organs. *Front. Plant Sci.* 7: 276.

800 Abraham, P.E., Garcia, B.J., Gunter, L.E., Jawdy, S.S., Engle, N., Yang, X., Jacobson, D.A.,
801 Hettich, R.L., Tuskan, G.A., and Tschaplinski, T.J. (2018). Quantitative proteome profile of
802 water deficit stress responses in eastern cottonwood (*Populus deltoides*) leaves. *PLoS One*
803 13: e0190019.

804 Aibar, S., Gonzalez-Blas, C.B., Moerman, T., Huynh-Thu, V.A., Imrichova, H., Hulselmans,
805 G., Rambow, F., Marine, J.C., Geurts, P., Aerts, J., et al. (2017). SCENIC: single-cell
806 regulatory network inference and clustering. *Nat. Methods* 14: 1083-1086.

807 Arabidopsis Interactome Mapping Consortium (2011). Evidence for network evolution in an
808 Arabidopsis interactome map. *Science* 333: 601-607.

809 Ariel, F.D., Manavella, P.A., Dezar, C.A., and Chan, R.L. (2007). The true story of the HD-Zip
810 family. *Trends Plant Sci.* 12: 419-426.

811 Aroca, R., Porcel, R., and Ruiz-Lozano, J.M. (2012). Regulation of root water uptake under
812 abiotic stress conditions. *J. Exp. Bot.* 63: 43-57.

813 Asensi-Fabado, M.A., Amtmann, A., and Perrella, G. (2017). Plant responses to abiotic
814 stress: The chromatin context of transcriptional regulation. *Biochim. Biophys. Acta* 1860: 106-
815 122.

816 Auguie, B. (2017). gridExtra: Miscellaneous Functions for "Grid" Graphics.

817 Battaglia, M., Olvera-Carrillo, Y., Garcarrubio, A., Campos, F., and Covarrubias, A.A. (2008).
818 The enigmatic LEA proteins and other hydrophilins. *Plant Physiol.* 148: 6-24.

819 Berardini, T.Z., Reiser, L., Li, D., Mezheritsky, Y., Muller, R., Strait, E., and Huala, E. (2015).
820 The Arabidopsis information resource: Making and mining the "gold standard" annotated
821 reference plant genome. *Genesis* 53: 474-485.

822 Bi, Z., Merl-Pham, J., Uehlein, N., Zimmer, I., Mühlhans, S., Aichler, M., Walch, A.K.,
823 Kaldenhoff, R., Palme, K., Schnitzler, J.P., et al. (2015). RNAi-mediated downregulation of

824 poplar plasma membrane intrinsic proteins (PIPs) changes plasma membrane proteome
825 composition and affects leaf physiology. *J. Proteomics* 128: 321-332.

826 Bloemen, J., Vergeynst, L.L., Overlaet-Michiels, L., and Steppe, K. (2016). How important is
827 woody tissue photosynthesis in poplar during drought stress? *Trees* 30: 63-72.

828 Challa, K.R., Aggarwal, P., and Nath, U. (2016). Activation of YUCCA5 by the transcription
829 factor TCP4 integrates developmental and environmental signals to promote hypocotyl
830 elongation in *Arabidopsis*. *Plant Cell* 28: 2217-2130.

831 Chen, J., Zhang, D., Zhang, C., Xia, X., Yin, W., and Tian, Q. (2015). A Putative PP2C-
832 Encoding Gene Negatively Regulates ABA Signaling in *Populus euphratica*. *PLoS One* 10:
833 e0139466.

834 Crisp, P.A., Ganguly, D., Eichten, S.R., Borevitz, J.O., and Pogson, B.J. (2016).
835 Reconsidering plant memory: Intersections between stress recovery, RNA turnover, and
836 epigenetics. *Sci. Adv.* 2: e1501340.

837 Csardi, G., and Nepusz, T. (2006). The igraph software package for complex network
838 research. *InterJournal Complex Systems*: 1695.

839 Ding, Y., Fromm, M., and Avramova, Z. (2012). Multiple exposures to drought 'train'
840 transcriptional responses in *Arabidopsis*. *Nat. Commun.* 3: 740.

841 Ding, Y., Liu, N., Virilouvet, L., Riethoven, J.J., Fromm, M., and Avramova, Z. (2013). Four
842 distinct types of dehydration stress memory genes in *Arabidopsis thaliana*. *BMC Plant Biol.*
843 13: 229.

844 Dong, C.J., and Liu, J.Y. (2010). The *Arabidopsis* EAR-motif-containing protein RAP2.1
845 functions as an active transcriptional repressor to keep stress responses under tight control.
846 *BMC Plant Biol.* 10: 47.

847 Dupeux, F., Antoni, R., Betz, K., Santiago, J., Gonzalez-Guzman, M., Rodriguez, L., Rubio,
848 S., Park, S.Y., Cutler, S.R., Rodriguez, P.L., et al. (2011). Modulation of abscisic acid
849 signaling in vivo by an engineered receptor-insensitive protein phosphatase type 2C allele.
850 *Plant Physiol.* 156: 106-116.

851 Dusa, A. (2018). venn: Draw Venn Diagrams.

852 Fleta-Soriano, E. and Munne-Bosch, S. (2016). Stress Memory and the inevitable effects of
853 drought: a physiological perspective. *Front. Plant Sci.* 7: 143.

854 Fox, J., and Weisberg, S. (2011). *An R Companion to Applied Regression* (Sage).

855 Fuchs, S., Grill, E., Meskiene, I., and Schweighofer, A. (2013). Type 2C protein phosphatases
856 in plants. *FEBS J.* 280: 681-693.

857 Fujii, H., Verslues, P.E., and Zhu, J.K. (2011). Arabidopsis decuple mutant reveals the
858 importance of SnRK2 kinases in osmotic stress responses *in vivo*. Proc. Natl. Acad. Sci. U. S.
859 A. 108: 1717-1722.

860 Gansner, E.R., and North, S.C. (2000). An open graph visualization system and its
861 applications to software engineering. SOFTWARE - PRACTICE AND EXPERIENCE 30:
862 1203-1233.

863 Gao, S., Gao, J., Zhu, X., Song, Y., Li, Z., Ren, G., Zhou, X., and Kuai, B. (2016). ABF2,
864 ABF3, and ABF4 promote ABA-mediated chlorophyll degradation and leaf senescence by
865 transcriptional activation of chlorophyll catabolic genes and senescence-associated genes in
866 Arabidopsis. Mol Plant 9: 1272-1285.

867 Gonzalez, I., Le Cao, K.A., and Dejean, S. (2011). mixOmics: Omics data integration project.

868 Goodstein, D.M., Shu, S., Howson, R., Neupane, R., Hayes, R.D., Fazo, J., Mitros, T., Dirks,
869 W., Hellsten, U., Putnam, N., et al. (2012). Phytozome: a comparative platform for green plant
870 genomics. Nucleic Acids Res. 40: D1178-1186.

871 Hagedorn, F., Joseph, J., Peter, M., Luster, J., Pritsch, K., Geppert, U., Kerner, R., Molinier,
872 V., Egli, S., Schaub, M., et al. (2016). Recovery of trees from drought depends on
873 belowground sink control. Nat. Plants 2: 16111.

874 Harfouche, A., Meilan, R., and Altman, A. (2014). Molecular and physiological responses to
875 abiotic stress in forest trees and their relevance to tree improvement. Tree Physiol 34: 1181-
876 1198.

877 Hilker, M., Schwachtje, J., Baier, M., Balazadeh, S., Baurle, I., Geiselhardt, S., Hinch, D.K.,
878 Kunze, R., Mueller-Roeber, B., Rillig, M.C., et al. (2016). Priming and memory of stress
879 responses in organisms lacking a nervous system. Biol. Rev. Camb. Philos. Soc. 91: 1118-
880 1133.

881 Hjellström, M., Olsson, A.S.B., Engström, O., and Söderman, E.M. (2003). Constitutive
882 expression of the water deficit-inducible homeobox gene ATHB7 in transgenic Arabidopsis
883 causes a suppression of stem elongation growth. Plant Cell Environ. 26: 1127-1136.

884 Huynh-Thu, V.A., Irrthum, A., Wehenkel, L., and Geurts, P. (2010). Inferring regulatory
885 networks from expression data using tree-based methods. PLoS One 5.

886 International Barley Genome Sequencing Consortium, Mayer, K.F., Waugh, R., Brown, J.W.,
887 Schulman, A., Langridge, P., Platzer, M., Fincher, G.B., Muehlbauer, G.J., Sato, K., et al.
888 (2012). A physical, genetic and functional sequence assembly of the barley genome. Nature
889 491: 711-716.

890 IPCC (2014). Near-term Climate Change: Projections and Predictability. In Climate Change
891 2013: The Physical Science Basis. Contribution of Working Group I to the Fifth Assessment
892 Report of the Intergovernmental Panel on Climate Change, T.F. Stocker, D. Qin, G.K.
893 Plattner, M. Tignor, S.K. Allen, J. Boschung, A. Nauels, Y. Xia, B. V., and P.M. Midgley, eds.
894 (Cambridge: Cambridge University Press).

895 Jin, J., Zhang, H., Kong, L., Gao, G., and Luo, J. (2014). PlantTFDB 3.0: a portal for the
896 functional and evolutionary study of plant transcription factors. *Nucleic Acids Res.* 42: D1182-
897 1187.

898 Jud, W., Vanzo, E., Li, Z., Ghirardo, A., Zimmer, I., Sharkey, T.D., Hansel, A., and Schnitzler,
899 J.P. (2016). Effects of heat and drought stress on post-illumination bursts of volatile organic
900 compounds in isoprene-emitting and non-emitting poplar. *Plant Cell Environ.* 39: 1204-1215.

901 Kim, D., Pertea, G., Trapnell, C., Pimentel, H., Kelley, R., and Salzberg, S.L. (2013).
902 TopHat2: accurate alignment of transcriptomes in the presence of insertions, deletions and
903 gene fusions. *Genome Biol.* 14: R36.

904 Kim, M., Lee, U., Small, I., des Francs-Small, C.C., and Vierling, E. (2012). Mutations in an
905 Arabidopsis mitochondrial transcription termination factor-related protein enhance
906 thermotolerance in the absence of the major molecular chaperone HSP101. *Plant Cell* 24:
907 3349-3365.

908 Kolde, R. (2018). pheatmap: Pretty Heatmaps.

909 Kotak, S., Larkindale, J., Lee, U., von Koskull-Doring, P., Vierling, E., and Scharf, K.D. (2007).
910 Complexity of the heat stress response in plants. *Curr. Opin. Plant Biol.* 10: 310-316.

911 Kulik, A., Wawer, I., Krzywinska, E., Bucholc, M., and Dobrowolska, G. (2011). SnRK2 protein
912 kinases--key regulators of plant response to abiotic stresses. *OMICS* 15: 859-872.

913 Lämke, J., Brzezinka, K., Altmann, S., and Bäurle, I. (2016). A hit-and-run heat shock factor
914 governs sustained histone methylation and transcriptional stress memory. *EMBO J.* 35: 162-
915 175.

916 Langfelder, P., and Horvath, S. (2007). Eigengene networks for studying the relationships
917 between co-expression modules. *BMC Syst. Biol.* 1: 54.

918 Langfelder, P., and Horvath, S. (2008). WGCNA: an R package for weighted correlation
919 network analysis. *BMC Bioinformatics* 9: 559.

920 Langfelder, P., and Horvath, S. (2012). Fast R Functions for Robust Correlations and
921 Hierarchical Clustering. *J Stat Softw* 46.

922 Langfelder, P., Zhang, B., and Horvath, S. (2008). Defining clusters from a hierarchical cluster
923 tree: the dynamic tree cut package for R. *Bioinformatics* 24: 719-720.

924 Le Cao, K.A., Gonzalez, I., and Dejean, S. (2009). integrOmics: an R package to unravel
925 relationships between two omics datasets. *Bioinformatics* 25: 2855-2856.

926 Leonhardt, N., Kwak, J.M., Robert, N., Waner, D., Leonhardt, G., and Schroeder, J.I. (2004).
927 Microarray expression analyses of Arabidopsis guard cells and isolation of a recessive
928 abscisic acid hypersensitive protein phosphatase 2C mutant. *Plant Cell* 16: 596-615.

929 Lepié, J.C., Brasileiro, A.C., Michel, M.F., Delmotte, F., and Jouanin, L. (1992). Transgenic
930 poplars: expression of chimeric genes using four different constructs. *Plant Cell Rep.* 11: 137-
931 141.

932 Li, S. (2014). Redox modulation matters: emerging functions for glutaredoxins in plant
933 development and stress responses. *Plants (Basel)* 3: 559-582.

934 Lippold, F., vom Dorp, K., Abraham, M., Holzl, G., Wewer, V., Yilmaz, J.L., Lager, I.,
935 Montandon, C., Besagni, C., Kessler, F., et al. (2012). Fatty acid phytol ester synthesis in
936 chloroplasts of Arabidopsis. *Plant Cell* 24: 2001-2014.

937 Liu, N., Staswick, P.E., and Avramova, Z. (2016). Memory responses of jasmonic acid-
938 associated Arabidopsis genes to a repeated dehydration stress. *Plant Cell Environ.* 39: 2515-
939 2529.

940 Love, M.I., Huber, W., and Anders, S. (2014). Moderated estimation of fold change and
941 dispersion for RNA-seq data with DESeq2. *Genome Biol.* 15: 550.

942 Mi, H., Huang, X., Muruganujan, A., Tang, H., Mills, C., Kang, D., and Thomas, P.D. (2017).
943 PANTHER version 11: expanded annotation data from Gene Ontology and Reactome
944 pathways, and data analysis tool enhancements. *Nucleic Acids Res.* 45: D183-D189.

945 Nakashima, K., Fujita, Y., Kanamori, N., Katagiri, T., Umezawa, T., Kidokoro, S., Maruyama,
946 K., Yoshida, T., Ishiyama, K., Kobayashi, M., et al. (2009). Three Arabidopsis SnRK2 protein
947 kinases, SRK2D/SnRK2.2, SRK2E/SnRK2.6/OST1 and SRK2I/SnRK2.3, involved in ABA
948 signaling are essential for the control of seed development and dormancy. *Plant Cell Physiol.*
949 50: 1345-1363.

950 Nakashima, K., Yamaguchi-Shinozaki, K., and Shinozaki, K. (2014). The transcriptional
951 regulatory network in the drought response and its crosstalk in abiotic stress responses
952 including drought, cold, and heat. *Front. Plant Sci.* 5: 170.

953 Olvera-Carrillo, Y., Campos, F., Reyes, J.L., Garcarrubio, A., and Covarrubias, A.A. (2010).
954 Functional analysis of the group 4 late embryogenesis abundant proteins reveals their

955 relevance in the adaptive response during water deficit in Arabidopsis. *Plant Physiol.* 154:
956 373-390.

957 Osakabe, Y., Osakabe, K., Shinozaki, K., and Tran, L.S. (2014). Response of plants to water
958 stress. *Front. Plant Sci.* 5: 86.

959 Paul, S., Wildhagen, H., Janz, D., and Polle, A. (2018). Drought effects on the tissue- and
960 cell-specific cytokinin activity in poplar. *AoB Plants* 10: plx067.

961 Perteau, M., Perteau, G.M., Antonescu, C.M., Chang, T.C., Mendell, J.T., and Salzberg, S.L.
962 (2015). StringTie enables improved reconstruction of a transcriptome from RNA-seq reads.
963 *Nat. Biotechnol.* 33: 290-295.

964 Pfanz, H., Aschan, G., Langenfeld-Heyser, R., Wittmann, C., and Loose, M. (2002). Ecology
965 and ecophysiology of tree stems: corticular and wood photosynthesis. *Naturwissenschaften*
966 89: 147-162.

967 R Core Team (2018). *R: A Language and Environment for Statistical Computing.*

968 Re, D.A., Capella, M., Bonaventure, G., and Chan, R.L. (2014). Arabidopsis AtHB7 and
969 AtHB12 evolved divergently to fine tune processes associated with growth and responses to
970 water stress. *BMC Plant Biol.* 14: 150.

971 Samol, I., Shapiguzov, A., Ingelsson, B., Fucile, G., Crevecoeur, M., Vener, A.V., Rochaix,
972 J.D., and Goldschmidt-Clermont, M. (2012). Identification of a photosystem II phosphatase
973 involved in light acclimation in Arabidopsis. *Plant Cell* 24: 2596-2609.

974 Sani, E., Herzyk, P., Perrella, G., Colot, V., and Amtmann, A. (2013). Hyperosmotic priming of
975 Arabidopsis seedlings establishes a long-term somatic memory accompanied by specific
976 changes of the epigenome. *Genome Biol.* 14: R59.

977 Schäfer, J., and Strimmer, K. (2005). A shrinkage approach to large-scale covariance matrix
978 estimation and implications for functional genomics. *Stat. Appl. Genet. Mol. Biol.* 4: Article32.

979 Scholander, P.F., Bradstreet, E.D., Hemmingsen, E.A., and Hammel, H.T. (1965). Sap
980 pressure in vascular plants: negative hydrostatic pressure can be measured in plants.
981 *Science* 148: 339-346.

982 Shinozaki, K., and Yamaguchi-Shinozaki, K. (2007). Gene networks involved in drought
983 stress response and tolerance. *J. Exp. Bot.* 58: 221-227.

984 Singh, D., and Laxmi, A. (2015). Transcriptional regulation of drought response: a tortuous
985 network of transcriptional factors. *Front. Plant Sci.* 6: 895.

986 Söderman, E., Mattsson, J., and Engström, P. (1996). The Arabidopsis homeobox gene
987 ATHB-7 is induced by water deficit and by abscisic acid. *Plant J.* 10: 375-381.

988 Soy, J., Leivar, P., Gonzalez-Schain, N., Sentandreu, M., Prat, S., Quail, P.H., and Monte, E.
989 (2012). Phytochrome-imposed oscillations in PIF3 protein abundance regulate hypocotyl
990 growth under diurnal light/dark conditions in *Arabidopsis*. *Plant J.* 71: 390-401.

991 Sun, X., Wang, C., Xiang, N., Li, X., Yang, S., Du, J., Yang, Y., and Yang, Y. (2017).
992 Activation of secondary cell wall biosynthesis by miR319-targeted TCP4 transcription factor.
993 *Plant Biotechnol. J.* 15: 1284-1294.

994 Sundell, D., Street, N.R., Kumar, M., Mellerowicz, E.J., Kucukoglu, M., Johnsson, C., Kumar,
995 V., Mannapperuma, C., Delhomme, N., Nilsson, O., et al. (2017). AspWood: High-spatial-
996 resolution transcriptome profiles reveal uncharacterized modularity of wood formation in
997 *Populus tremula*. *Plant Cell* 29: 1585-1604.

998 Tan, Q.K., and Irish, V.F. (2006). The *Arabidopsis* zinc finger-homeodomain genes encode
999 proteins with unique biochemical properties that are coordinately expressed during floral
1000 development. *Plant Physiol.* 140: 1095-1108.

1001 Taylor, G. (2002). *Populus: arabidopsis for forestry*. Do we need a model tree? *Ann. Bot.* 90:
1002 681-689.

1003 Thiel, S., Döhring, T., Köfferlein, M., Kosak, A., Martin, P., and Seidlitz, H.K. (1996) A
1004 phytotron for plant stress research: How far can artificial lighting compare to natural sunlight?
1005 *J. Plant Physiol.* 148: 456–463.

1006 Tischer, S.V., Wunschel, C., Papacek, M., Kleigrew, K., Hofmann, T., Christmann, A., and
1007 Grill, E. (2017). Combinatorial interaction network of abscisic acid receptors and coreceptors
1008 from *Arabidopsis thaliana*. *Proc. Natl. Acad. Sci. U. S. A.* 114: 10280-10285.

1009 Tran, L.S., Nakashima, K., Sakuma, Y., Osakabe, Y., Qin, F., Simpson, S.D., Maruyama, K.,
1010 Fujita, Y., Shinozaki, K., and Yamaguchi-Shinozaki, K. (2007). Co-expression of the stress-
1011 inducible zinc finger homeodomain ZFHD1 and NAC transcription factors enhances
1012 expression of the ERD1 gene in *Arabidopsis*. *Plant J.* 49: 46-63.

1013 Tran, L.S., Nakashima, K., Sakuma, Y., Simpson, S.D., Fujita, Y., Maruyama, K., Fujita, M.,
1014 Seki, M., Shinozaki, K., and Yamaguchi-Shinozaki, K. (2004). Isolation and functional analysis
1015 of *Arabidopsis* stress-inducible NAC transcription factors that bind to a drought-responsive
1016 cis-element in the early responsive to dehydration stress 1 promoter. *Plant Cell* 16: 2481-
1017 2498.

1018 Tuskan, G.A., Difazio, S., Jansson, S., Bohlmann, J., Grigoriev, I., Hellsten, U., Putnam, N.,
1019 Ralph, S., Rombauts, S., Salamov, A., et al. (2006). The genome of black cottonwood,
1020 *Populus trichocarpa* (Torr. & Gray). *Science* 313: 1596-1604.

1021 Valdés, A.E., Overnäs, E., Johansson, H., Rada-Iglesias, A., and Engström, P. (2012). The
1022 homeodomain-leucine zipper (HD-Zip) class I transcription factors ATHB7 and ATHB12
1023 modulate abscisic acid signalling by regulating protein phosphatase 2C and abscisic acid
1024 receptor gene activities. *Plant Mol. Biol.* 80: 405-418.

1025 Vanzo, E., Jud, W., Li, Z., Albert, A., Domagalska, M.A., Ghirardo, A., Niederbacher, B.,
1026 Frenzel, J., Beemster, G.T., Asard, H., et al. (2015). Facing the future: effects of short-term
1027 climate extremes on isoprene-emitting and non-emitting poplar. *Plant Physiol.* 169: 560-575.

1028 von Caemmerer, S., and Farquhar, G.D. (1981). Some relationships between the
1029 biochemistry of photosynthesis and the gas exchange of leaves. *Planta* 153: 376-387.

1030 Wang, L., Hua, D., He, J., Duan, Y., Chen, Z., Hong, X., and Gong, Z. (2011). Auxin
1031 Response Factor2 (ARF2) and its regulated homeodomain gene HB33 mediate abscisic acid
1032 response in *Arabidopsis*. *PLoS Genet.* 7: e1002172.

1033 Wang, X., Vignjevic, M., Jiang, D., Jacobsen, S., and Wollenweber, B. (2014). Improved
1034 tolerance to drought stress after anthesis due to priming before anthesis in wheat (*Triticum*
1035 *aestivum* L.) var. Vinjett. *J. Exp. Bot.* 65: 6441-6456.

1036 Warnes, G.R., Bolker, B., Bonebakker, L., Gentleman, R., Huber, W., Liaw, A., Lumley, T.,
1037 Maechler, M., Magnusson, A., Moeller, S., et al. (2016). *gplots: Various R Programming*
1038 *Tools for Plotting Data.*

1039 Wickham, H. (2009). *ggplot2: Elegant Graphics for Data Analysis* (Springer-Verlag New
1040 York).

1041 Wildhagen, H., Paul, S., Allwright, M., Smith, H.K., Malinowska, M., Schnabel, S.K., Paulo,
1042 M.J., Cattonaro, F., Vendramin, V., Scalabrin, S., et al. (2018). Genes and gene clusters
1043 related to genotype and drought-induced variation in saccharification potential, lignin content
1044 and wood anatomical traits in *Populus nigra*. *Tree Physiol* 38: 320-339.

1045 Xu, Z., Zhou, G., and Shimizu, H. (2010). Plant responses to drought and rewatering. *Plant*
1046 *Signal. Behav.* 5: 649-654.

1047 Yao, W., Zhang, X., Zhou, B., Zhao, K., Li, R., and Jiang, T. (2017). Expression pattern of
1048 ERF gene family under multiple abiotic stresses in *Populus simonii* x *P. nigra*. *Front. Plant*
1049 *Sci.* 8: 181.

1050 Yazaki, J., Galli, M., Kim, A.Y., Nito, K., Aleman, F., Chang, K.N., Carvunis, A.R., Quan, R.,
1051 Nguyen, H., Song, L., et al. (2016). Mapping transcription factor interactome networks using
1052 HaloTag protein arrays. *Proc. Natl. Acad. Sci. U. S. A.* 113: E4238-4247.

1053 Yu, J., Yang, L., Liu, X., Tang, R., Wang, Y., Ge, H., Wu, M., Zhang, J., Zhao, F., Luan, S., et
1054 al. (2016). Overexpression of poplar pyrabactin resistance-like abscisic acid receptors
1055 promotes abscisic acid sensitivity and drought resistance in transgenic Arabidopsis. PLoS
1056 One 11: e0168040.

1057 Zhang, K., and Gan, S.S. (2012). An abscisic acid-AtNAP transcription factor-SAG113 protein
1058 phosphatase 2C regulatory chain for controlling dehydration in senescing Arabidopsis leaves.
1059 Plant Physiol. 158: 961-969.

1060 Zhong, S., Shi, H., Xue, C., Wang, L., Xi, Y., Li, J., Quail, P.H., Deng, X.W., and Guo, H.
1061 (2012). A molecular framework of light-controlled phytohormone action in Arabidopsis. Curr.
1062 Biol. 22: 1530-1535.

1063

1064 **FIGURE LEGENDS**

1065 **Figure 1. Effect of climatic stress on the post-recovery photosynthetic performance of**
1066 **poplar trees.** (A) The 3D experimental design to investigate the climate response of *P. ×*
1067 *canescens* trees regarding memory aspects and systemic effects. Plants from four
1068 environmental conditions including the ambient CO₂ control (AC), enhanced CO₂ control (EC),
1069 periodic drought-heat stress (PS) and chronic drought-heat stress (CS) were examined both
1070 at the end of a 22-day (d22) stress phase (S) and after one week of recovery (R). At the start
1071 of the stress treatment (d0), the plants were 8.5 weeks old and already under AC and EC
1072 control climates for 25 days. For fully developed leaves, both phenotypic and transcriptomic
1073 measurements are available; only transcriptomic data are available for the four other tissues.

1074 (B-D) Comparison of leaf-level gas exchange rates (leaf no. 9 from the apex) across
1075 environmental conditions (center line, median; box limits, upper and lower quartiles; whiskers,
1076 maximum and minimum). For each of the two phases (separated by the vertical line), groups
1077 that do not share identical lowercase letters are significantly different (Kruskal-Wallis test with
1078 posthoc Dunn's test, Benjamini-Hochberg adjustment, p.adj<0.05). (E) Carbon gain
1079 determined by online gas exchange analysis for the gas-tight sub-chamber of each
1080 environmental condition. The slope (shown by circles) was estimated from the last four
1081 measurements (day 26 to day 29). Different lowercase letters indicate a significant difference
1082 of slopes (Kruskal-Wallis test with posthoc Dunn's test, Benjamini-Hochberg adjustment,
1083 p.adj<0.05). (F) Projection on the top two components from canonical correlation analysis
1084 between gas exchange data and log₂(TPM+1)-transformed per-gene RNA-seq data of the
1085 100 most varying genes in mature leaves across the four conditions and two treatment

1086 phases. Each data point represents the mean of biological replicates for the given group; due
1087 to destructive harvesting, stress phase RNA-seq measurements were obtained from different
1088 biological samples from the continuous gas exchange measurements. Ellipses mark 0.75
1089 confidence levels estimated from the replicates.

1090

1091 **Figure 2. System-wide comparison of poplar gene expression under stress, recovery**
1092 **and control conditions.** (A) Projection on top two components from principal component
1093 analysis of $\log_2(\text{TPM}+1)$ -transformed per-gene RNA-seq data from all samples across four
1094 climate conditions, two treatment phases, five different tissues and three biological replicates
1095 per group. The biological replicates are tissue samples from different trees subjected to the
1096 same environmental condition and harvested at the same time. Data points are colored by
1097 tissue (LE1: young leaves, LE2: mature leaves, PHL: phloem, XYL: xylem, ROO: root). (B)
1098 Principal component analysis of poplar trees with complete RNA-seq measurements from all
1099 five tissues, concatenating all tissue measurements from the same tree (see Methods).
1100 Ellipses mark the 0.75 confidence contour for stressed trees and all other trees (AC: ambient
1101 CO_2 , EC: enhanced CO_2 , PS: periodic stress, CS: chronic stress; S: stress phase, R:
1102 recovery phase). (C) Number of differentially expressed genes overlapping between periodic
1103 (PS) and chronic stress treatment (CS) or unique to each stress type. Differential expression
1104 was determined relative to untreated EC controls for each tissue and treatment phase
1105 separately (fold change > 2 , $p.\text{adj} < 0.05$). The dashed box shows a zoom-in for the three
1106 bottommost groups. (D) Comparison of antioxidant levels in mature leaves across
1107 environmental conditions. Groups that do not share identical lowercase letters are
1108 significantly different (Kruskal-Wallis test with posthoc Dunn's test, Benjamini-Hochberg
1109 adjustment, $p.\text{adj} < 0.05$). The y-axis gives the percentage of functional, reduced ascorbate
1110 relative to total ascorbate (oxidized and reduced forms). (E) Stress-recovery overlap of up-
1111 regulated genes. For each tissue, the percentage of stress phase down- or up-regulation of
1112 genes up-regulated in the recovery phase relative to control plants is given (fold change > 2 ,
1113 $p.\text{adj} < 0.05$).

1114

1115 **Figure 3. Tissue overlap of differentially expressed poplar genes during the stress and**
1116 **recovery phases.** Each Venn diagram gives the number of up- or down-regulated genes for
1117 a specific treatment type and a specific phase in comparison to untreated controls (LE1:

1118 young leaves, LE2: mature leaves, PHL: phloem, XYL: xylem, ROO: root; PS: periodic stress,
1119 CS: chronic stress; S: stress phase, R: recovery phase).

1120

1121 **Figure 4. Characteristic poplar gene expression profiles across stress, recovery and**
1122 **control conditions shared by all tissues.** Each network node represents a co-expression
1123 module of a specific tissue (see Methods), as indicated by the respective node color (identical
1124 code to Figure 2A) and the prefix of the node label (LE1: young leaves, LE2: mature leaves,
1125 PHL: phloem, XYL: xylem, ROO: root). Subsequent numbers in the node label identify the
1126 module within each tissue in decreasing order of module size, which is indicated by node
1127 size. Each module is represented by its eigengene profile, which is the first principal
1128 component oriented according to average expression. The correlation of module eigengenes
1129 was used to cluster the modules into communities (see Methods). The figure shows all
1130 communities that contain modules from all five tissues together with heatmaps of the
1131 corresponding eigengenes. Communities are marked by gray polygons and C identifiers
1132 (decreasing shades of gray with increasing identifier numbers). For correlation values > 0.7 ,
1133 edges are depicted between module nodes and the edge width represents the correlation
1134 strength. The heatmaps with background shading exhibit a pronounced difference between
1135 stress-exposed plants and non-treated plants at the end of the recovery phase for at least one
1136 stress type, indicative of stress-related memory (EC: elevated CO₂ control, CS: chronic
1137 stress, PS: periodic stress; S: stress phase, R: recovery phase). Community C9 putatively
1138 represents age-related changes that only occur in non-stressed plants.

1139

1140 **Figure 5. Gene expression memory after recovery from periodic vs. chronic stress.** (A)
1141 Poplar genes with cross-tissue memory responses, i.e. transcriptional up- or down-regulation
1142 in post-recovery stress relative to enhanced CO₂ (EC) control samples. The heatmap shows
1143 periodic stress (PS) and chronic stress (CS) expression patterns of all genes with PS memory
1144 responses in at least two tissues (LE1: young leaves, LE2: mature leaves, PHL: phloem, XYL:
1145 xylem, ROO: root, R: recovery phase, S: stress phase). (B) Direct PS (R) vs. CS (R)
1146 comparison of differentially expressed recovery genes determined relative to the EC control
1147 (see A and Figure 2C). For each tissue, volcano plots show the distribution of overlapping and
1148 stress type-specific differential genes (left: down-regulation, right: up-regulation), taking
1149 adjusted p-values and fold changes from the direct comparison. Volcano plots for the
1150 respective PS vs. EC and CS vs. EC comparisons are available in Supplemental Figure 1.

1151

1152 **Figure 6. Expression self-correlation of genes across tissues based on fully sampled**
1153 **individual trees.** (A) The genes with the strongest self-correlation across all tissues. Among
1154 them are many genes with periodic stress memory expression patterns in at least one tissue,
1155 marked in black and annotated from top to bottom (letters a-q). (B) Heatmap showing the
1156 number of genes (see scale at the bottom) with self-correlation > 0.8 between individual
1157 tissues (LE1: young leaves, LE2: mature leaves, PHL: phloem, XYL: xylem, ROO: root).

1158

1159 **Figure 7. Gene regulatory networks of stress-related multi-tissue memory genes.** (A)
1160 Tissue-specific transcription factor networks around self-correlated genes (gray nodes,
1161 labeled by letter code from Figure 6A). For each tissue network, colored nodes and edges
1162 indicate their co-occurrence across several tissue networks (see color key). If nodes or edges
1163 occur only in one additional tissue (except the currently considered tissue indicated in the box
1164 at the top left of each network), they have the characteristic color of that additional tissue. For
1165 example, ten transcription factors occur only in the networks of both young and mature leaves
1166 (dark green and light green nodes in the first and second network, respectively). Likewise,
1167 nodes q and o are connected to the same transcription factor in these networks (dark green
1168 and light green edges in the first and second network, respectively). (B) Regulatory
1169 relationships co-occurring across tissues. The edge width is proportional to the number of
1170 tissues where a specific regulatory relationship was found. Transcription factor nodes are
1171 colored according to their transcription factor family.

1172

1173 **Figure 8. Predicted regulatory stress-related memory processes in mature leaves (LE2)**
1174 **and developing xylem (XYL).** (A) Core regulatory networks obtained by iteratively removing
1175 single-edge nodes from expression-based regulatory network predictions (Figure 7A). Node
1176 label colors refer to periodic stress-related expression patterns. Function annotation is shown
1177 for selected nodes discussed in the main text. Potri.010G193000 is a co-ortholog of the
1178 *Arabidopsis thaliana* MYB transcription factor AT5G05790, here abbreviated as MYB. (B)
1179 Model of possible transcription factor complex formation in stress-related memory derived
1180 from protein-protein interaction data in *Arabidopsis thaliana*. Gene names are taken from the
1181 orthology information in Phytozome. For some ZHD ortholog groups, different *Arabidopsis*
1182 genes (marked by an *Arabidopsis* ZHD identifier after the slash) constitute the best BLASTP
1183 matches of poplar genes. (C) Model suggesting physiological roles of protein phosphatases of

1184 type 2C (PP2Cs) and regulatory transcription factors in mature leaves during and after
1185 periodic stress.
1186

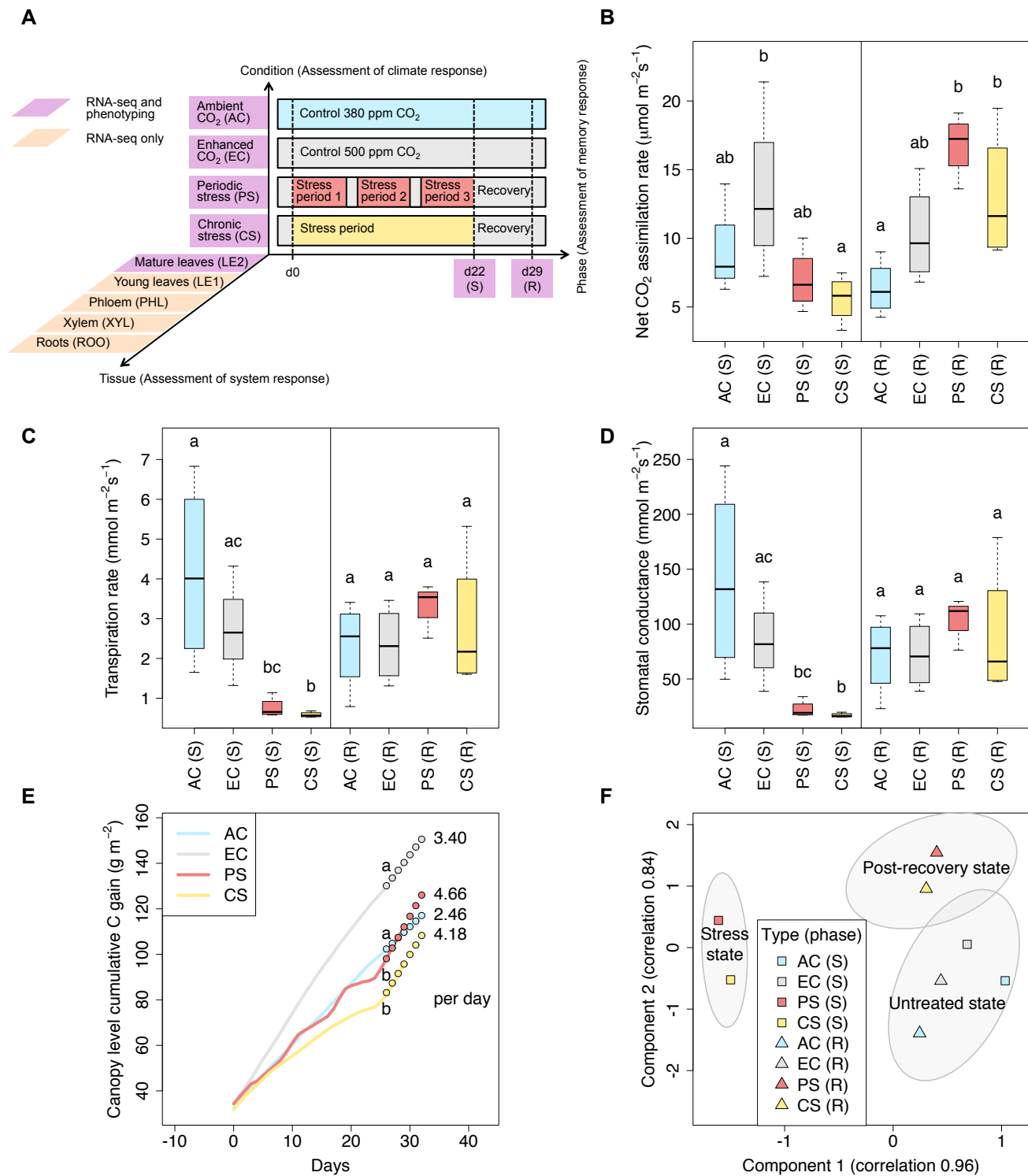


Figure 1. Effect of climatic stress on the post-recovery photosynthetic performance of poplar trees.

(A) The 3D experimental design to investigate the climate response of *P. × canescens* trees regarding memory aspects and systemic effects. Plants from four environmental conditions including the ambient CO₂ control (AC), enhanced CO₂ control (EC), periodic drought-heat stress (PS) and chronic drought-heat stress (CS) were examined both at the end of a 22-day (d22) stress phase (S) and after one week of recovery (R). At the start of the stress treatment (d0), the plants were 8.5 weeks old and already under AC and EC control climates for 25 days. For fully developed leaves, both phenotypic and transcriptomic measurements are available; only transcriptomic data are available for the four other tissues. (B-D) Comparison of leaf-level gas exchange rates (leaf no. 9 from the apex) across environmental conditions (center line, median; box limits, upper and lower quartiles; whiskers, maximum and minimum). For each of the two phases (separated by the vertical line), groups that do not share identical lowercase letters are significantly different (Kruskal-Wallis test with posthoc Dunn's test, Benjamini-Hochberg adjustment, p.adj<0.05). (E) Carbon gain determined by online gas exchange analysis for the gas-tight sub-chamber of each environmental condition. The slope (shown by circles) was estimated from the last four measurements (day 26 to day 29). Different lowercase letters indicate a significant difference of slopes (Kruskal-Wallis test with posthoc Dunn's test, Benjamini-Hochberg adjustment, p.adj<0.05). (F) Projection on the top two components from canonical correlation analysis between gas exchange data and log₂(TPM+1)-transformed per-gene RNA-seq data of the 100 most varying genes in mature leaves across the four conditions and two treatment phases. Each data point represents the mean of biological replicates for the given group; due to destructive harvesting, stress phase RNA-seq measurements were obtained from different biological samples from the continuous gas exchange measurements. Ellipses mark 0.75 confidence levels estimated from the replicates.

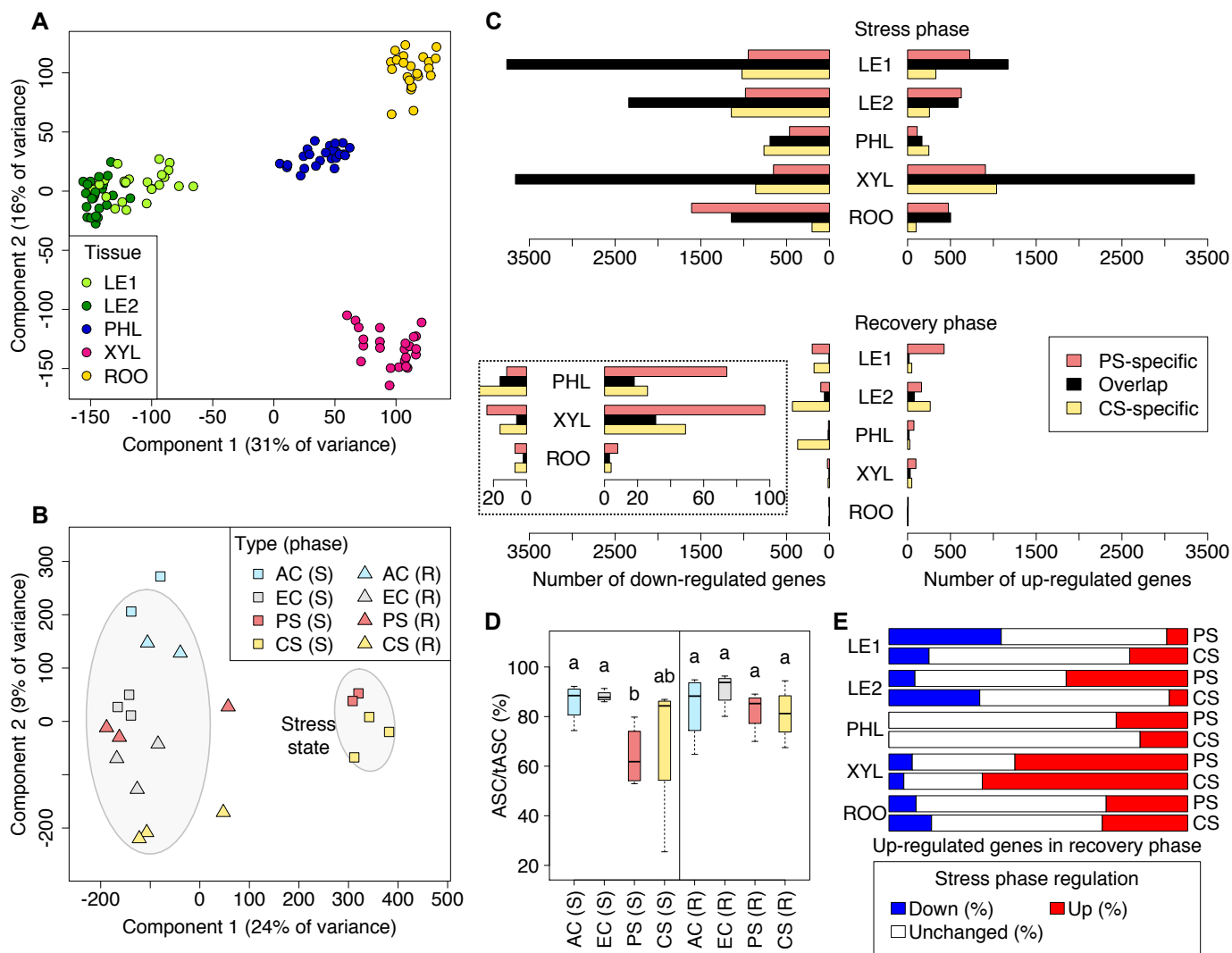


Figure 2. System-wide comparison of poplar gene expression under stress, recovery and control conditions. (A) Projection on top two components from principal component analysis of $\log_2(\text{TPM}+1)$ -transformed per-gene RNA-seq data from all samples across four climate conditions, two treatment phases, five different tissues and three biological replicates per group. The biological replicates are tissue samples from different trees subjected to the same environmental condition and harvested at the same time. Data points are colored by tissue (LE1: young leaves, LE2: mature leaves, PHL: phloem, XYL: xylem, ROO: root). (B) Principal component analysis of poplar trees with complete RNA-seq measurements from all five tissues, concatenating all tissue measurements from the same tree (see Methods). Ellipses mark the 0.75 confidence contour for stressed trees and all other trees (AC: ambient CO_2 , EC: enhanced CO_2 , PS: periodic stress, CS: chronic stress; S: stress phase, R: recovery phase). (C) Number of differentially expressed genes overlapping between periodic (PS) and chronic stress treatment (CS) or unique to each stress type. Differential expression was determined relative to untreated EC controls for each tissue and treatment phase separately (fold change > 2, $p_{\text{adj}} < 0.05$). The dashed box shows a zoom-in for the three bottommost groups. (D) Comparison of antioxidant levels in mature leaves across environmental conditions. Groups that do not share identical lowercase letters are significantly different (Kruskal-Wallis test with posthoc Dunn's test, Benjamini-Hochberg adjustment, $p_{\text{adj}} < 0.05$). The y-axis gives the percentage of functional, reduced ascorbate relative to total ascorbate (oxidized and reduced forms). (E) Stress-recovery overlap of up-regulated genes. For each tissue, the percentage of stress phase down- or up-regulation of genes up-regulated in the recovery phase relative to control plants is given (fold change > 2, $p_{\text{adj}} < 0.05$).

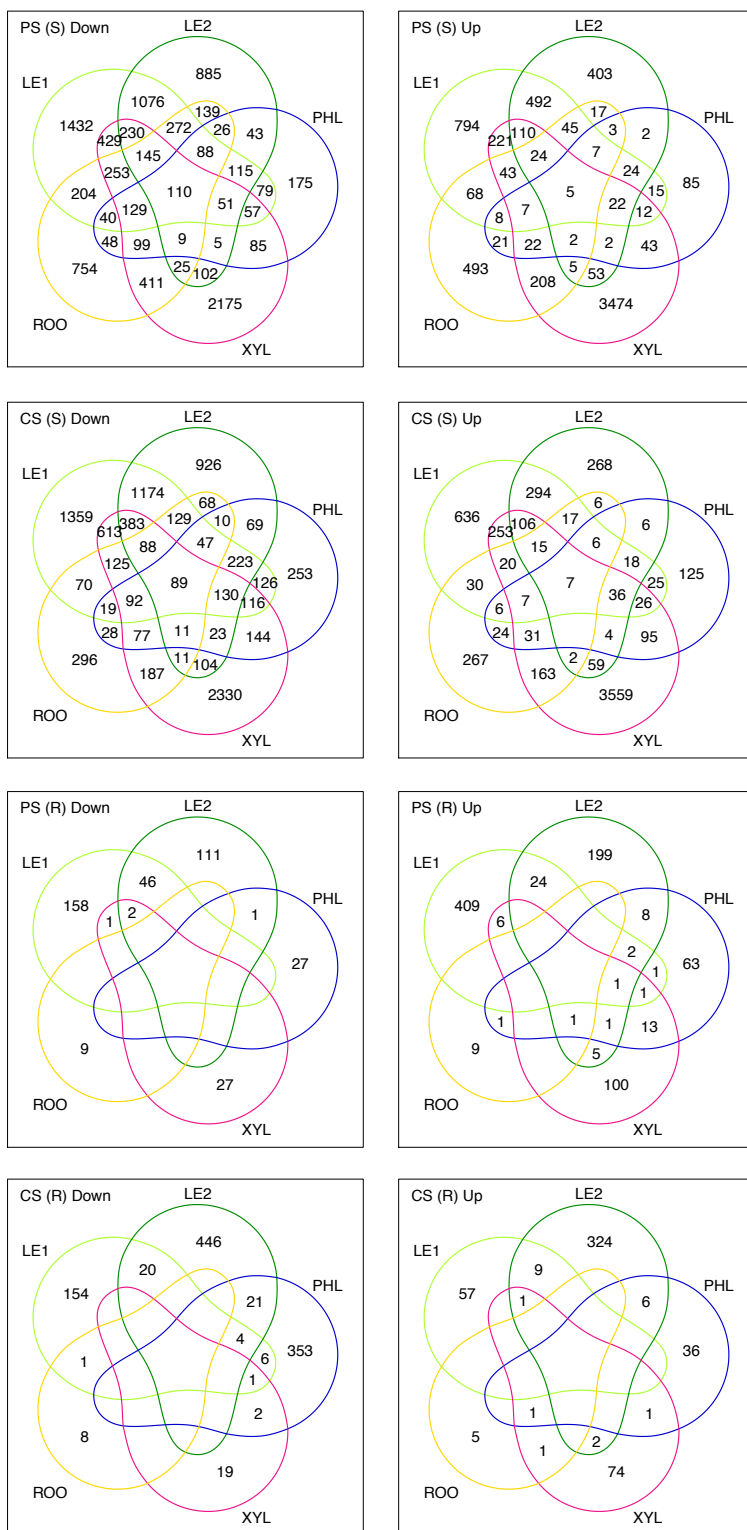


Figure 3. Tissue overlap of differentially expressed poplar genes during the stress and recovery phases. Each Venn diagram gives the number of up- or down-regulated genes for a specific treatment type and a specific phase in comparison to untreated controls (LE1: young leaves, LE2: mature leaves, PHL: phloem, XYL: xylem, ROO: root; PS: periodic stress, CS: chronic stress; S: stress phase, R: recovery phase).

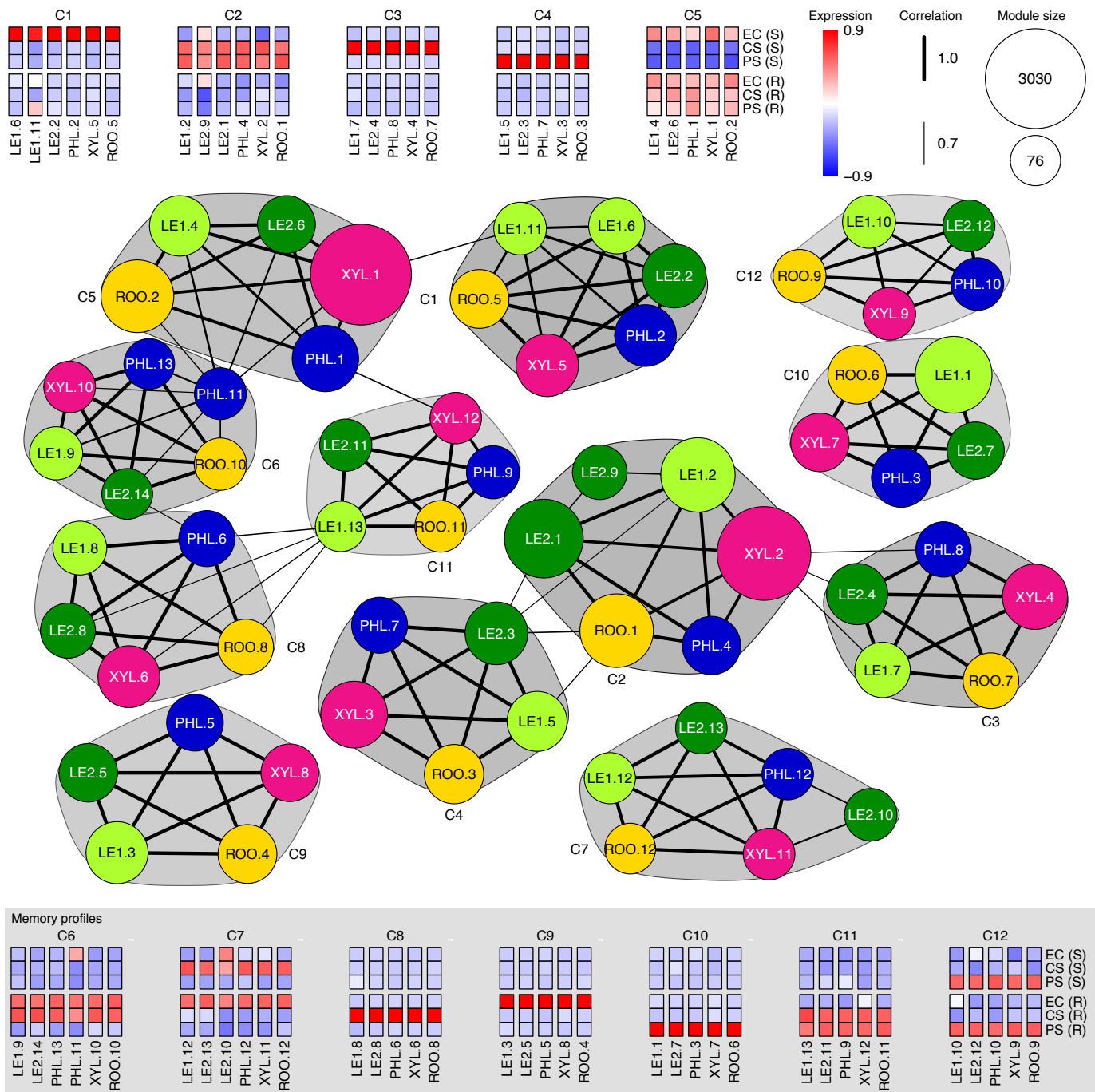
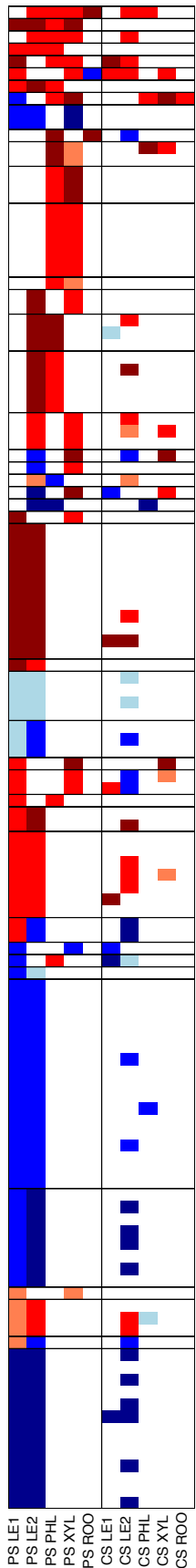
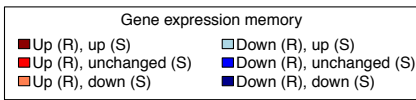


Figure 4. Characteristic poplar gene expression profiles across stress, recovery and control conditions shared by all tissues. Each network node represents a co-expression module of a specific tissue (see Methods), as indicated by the respective node color (identical code to Figure 2A) and the prefix of the node label (LE1: young leaves, LE2: mature leaves, PHL: phloem, XYL: xylem, ROO: root). Subsequent numbers in the node label identify the module within each tissue in decreasing order of module size, which is indicated by node size. Each module is represented by its eigengene profile, which is the first principal component oriented according to average expression. The correlation of module eigengenes was used to cluster the modules into communities (see Methods). The figure shows all communities that contain modules from all five tissues together with heatmaps of the corresponding eigengenes. Communities are marked by gray polygons and C identifiers (decreasing shades of gray with increasing identifier numbers). For correlation values > 0.7, edges are depicted between module nodes and the edge width represents the correlation strength. The heatmaps with background shading exhibit a pronounced difference between stress-exposed plants and non-treated plants at the end of the recovery phase for at least one stress type, indicative of stress-related memory (EC: elevated CO₂ control, CS: chronic stress, PS: periodic stress; S: stress phase, R: recovery phase). Community C9 putatively represents age-related changes that only occur in non-stressed plants.

A

Potri.005G174400
 Potri.017G009900
 Potri.010G199100
 Potri.004G115600
 Potri.014G106900
 Potri.003G029000
 Potri.003G112600
 Potri.018G139900
 Potri.012G122800
 Potri.017G148800
 Potri.010G150400
 Potri.012G141300
 Potri.015G109100
 Potri.006G093500
 Potri.011G139700
 Potri.013G018000
 Potri.001G192600
 Potri.003G193800
 Potri.005G078700
 Potri.009G151400
 Potri.012G041800
 Potri.014G000400
 Potri.003G141800
 Potri.001G083700
 Potri.012G082800
 Potri.003G131550
 Potri.004G073800
 Potri.013G009200
 Potri.004G074300
 Potri.008G059800
 Potri.008G121900
 Potri.010G184600
 Potri.010G191600
 Potri.001G239650
 Potri.001G239700
 Potri.015G004800
 Potri.003G159800
 Potri.002G220500
 Potri.016G001600
 Potri.008G212400
 Potri.002G094500
 Potri.007G109200
 Potri.001G092100
 Potri.003G129600
 Potri.004G044300
 Potri.005G094900
 Potri.005G129400
 Potri.006G052800
 Potri.008G096500
 Potri.009G107500
 Potri.010G157900
 Potri.010G201400
 Potri.019G131800
 Potri.004G074000
 Potri.001G359200
 Potri.002G027800
 Potri.005G215500
 Potri.009G035100
 Potri.001G019500
 Potri.001G354400
 Potri.010G086200
 Potri.007G088700
 Potri.002G054900
 Potri.006G234900
 Potri.001G235300
 Potri.006G115300
 Potri.011G003200
 Potri.001G099400
 Potri.001G190800
 Potri.003G047700
 Potri.006G089800
 Potri.010G152800
 Potri.0451062800
 Potri.015G097900
 Potri.014G043000
 Potri.009G140400
 Potri.001G408000
 Potri.007G133600
 Potri.003G006800
 Potri.001G347600
 Potri.002G075300
 Potri.003G074500
 Potri.003G089600
 Potri.005G090600
 Potri.009G035000
 Potri.009G044700
 Potri.010G029900
 Potri.010G135100
 Potri.012G008666
 Potri.014G005701
 Potri.014G086900
 Potri.015G096900
 Potri.016G019900
 Potri.017G075700
 Potri.017G083900
 Potri.004G102800
 Potri.005G196700
 Potri.006G127200
 Potri.008G135200
 Potri.010G105700
 Potri.015G002300
 Potri.015G140800
 Potri.017G079000
 Potri.008G100500
 Potri.005G257000
 Potri.006G255800
 Potri.009G005400
 Potri.004G070800
 Potri.001G082150
 Potri.004G072900
 Potri.004G155300
 Potri.007G072600
 Potri.008G131400
 Potri.009G116400
 Potri.012G005900
 Potri.013G119400
 Potri.016G002800
 Potri.016G028900
 Potri.018G142700
 Potri.019G034000
 Potri.T021500

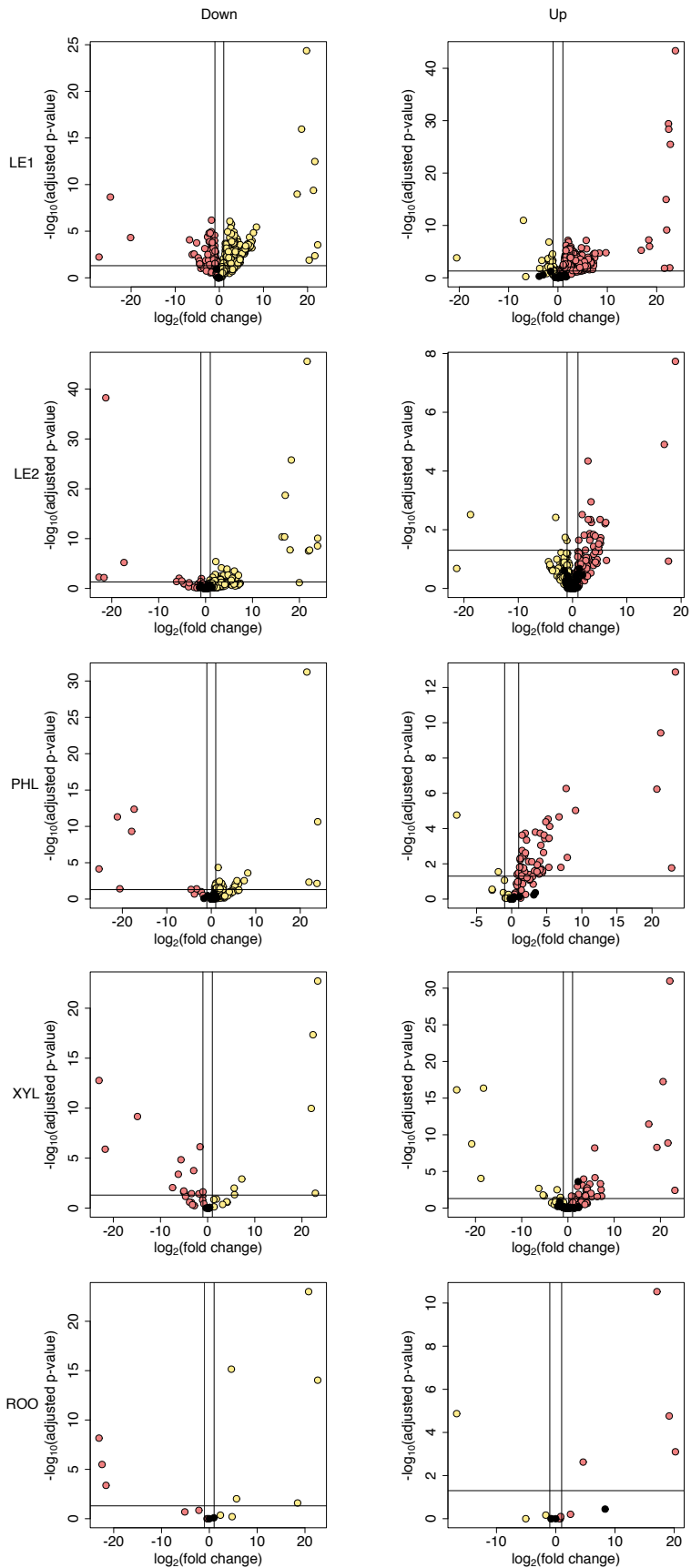
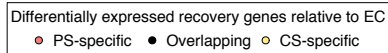
B

Figure 5. Gene expression memory after recovery from periodic vs. chronic stress. (A) Poplar genes with cross-tissue memory responses, i.e. transcriptional up- or down-regulation in post-recovery stress relative to enhanced CO₂ (EC) control samples. The heatmap shows periodic stress (PS) and chronic stress (CS) expression patterns of all genes with PS memory responses in at least two tissues (LE1: young leaves, LE2: mature leaves, PHL: phloem, XYL: xylem, ROO: root, R: recovery phase, S: stress phase). (B) Direct PS (R) vs. CS (R) comparison of differentially expressed recovery genes determined relative to the EC control (see A and Figure 2C). For each tissue, volcano plots show the distribution of overlapping and stress type-specific differential genes (left: down-regulation, right: up-regulation), taking adjusted p-values and fold changes from the direct comparison. Volcano plots for the respective PS vs. EC and CS vs. EC comparisons are available in Supplemental Figure 1.

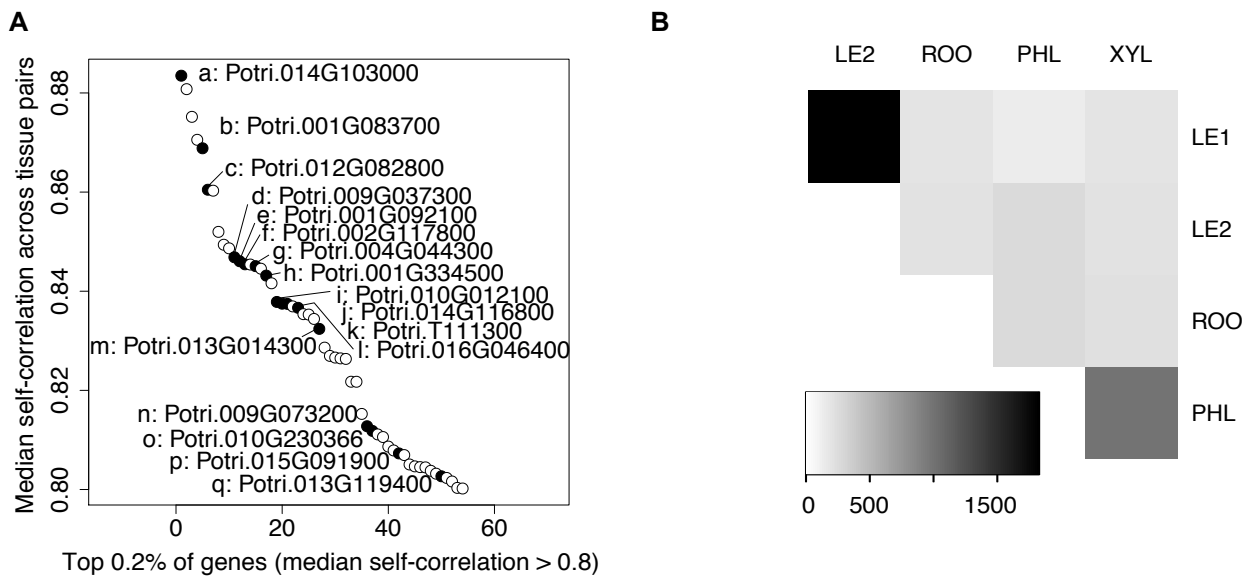


Figure 6. Expression self-correlation of genes across tissues based on fully sampled individual trees. (A) The genes with the strongest self-correlation across all tissues. Among them are many genes with periodic stress memory expression patterns in at least one tissue, marked in black and annotated from top to bottom (letters a-q). (B) Heatmap showing the number of genes (see scale at the bottom) with self-correlation > 0.8 between individual tissues (LE1: young leaves, LE2: mature leaves, PHL: phloem, XYL: xylem, ROO: root).

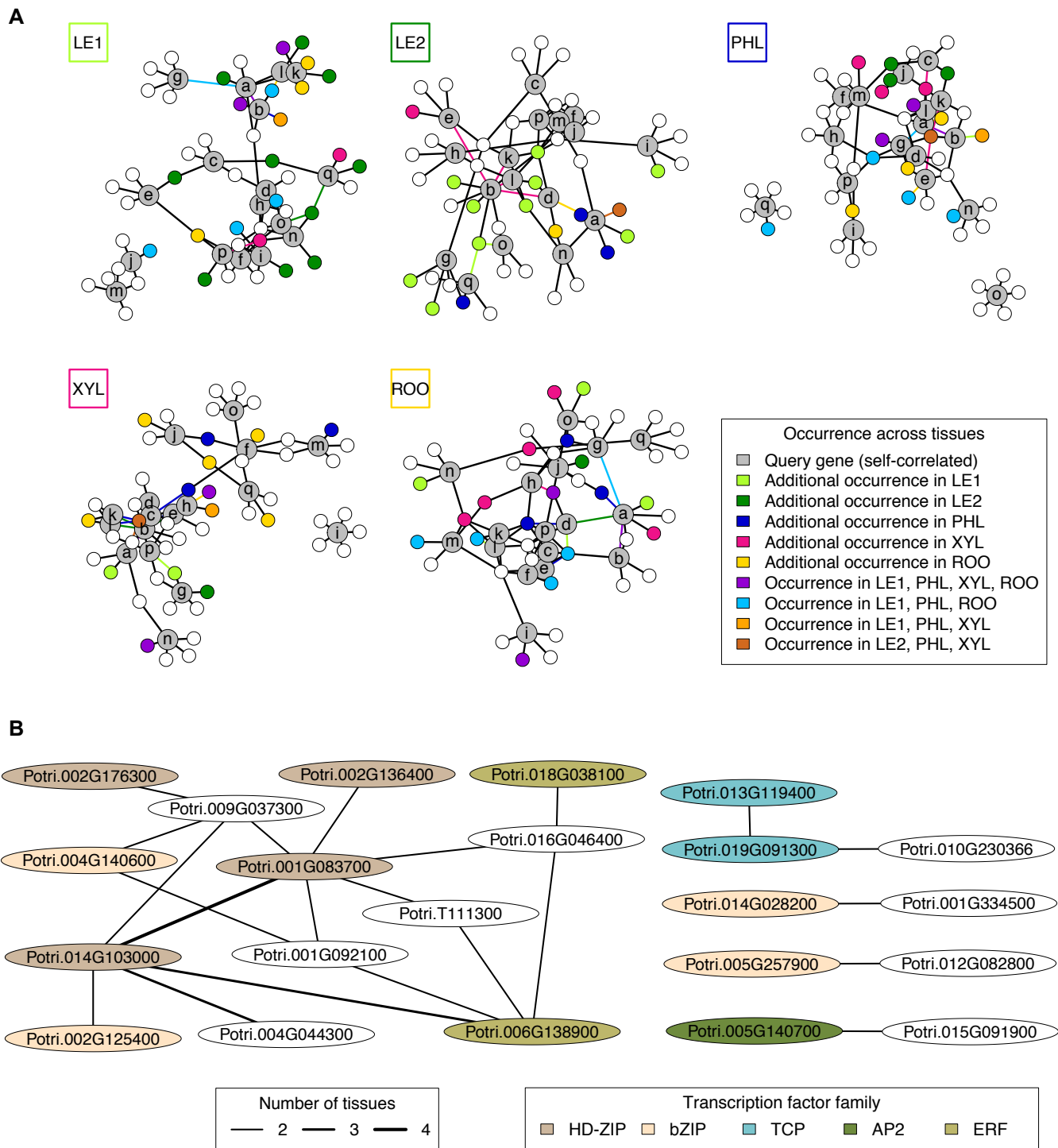


Figure 7. Gene regulatory networks of stress-related multi-tissue memory genes. (A) Tissue-specific transcription factor networks around self-correlated genes (gray nodes, labeled by letter code from Figure 6A). For each tissue network, colored nodes and edges indicate their co-occurrence across several tissue networks (see color key). If nodes or edges occur only in one additional tissue (except the currently considered tissue indicated in the box at the top left of each network), they have the characteristic color of that additional tissue. For example, ten transcription factors occur only in the networks of both young and mature leaves (dark green and light green nodes in the first and second network, respectively). Likewise, nodes q and o are connected to the same transcription factor in these networks (dark green and light green edges in the first and second network, respectively). (B) Regulatory relationships co-occurring across tissues. The edge width is proportional to the number of tissues where a specific regulatory relationship was found. Transcription factor nodes are colored according to their transcription factor family.

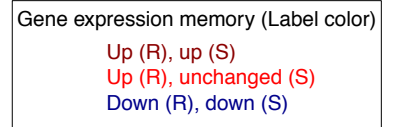
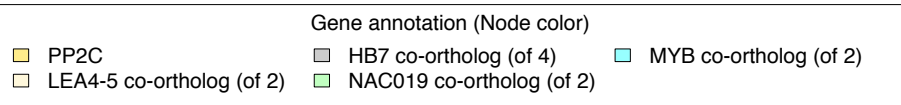
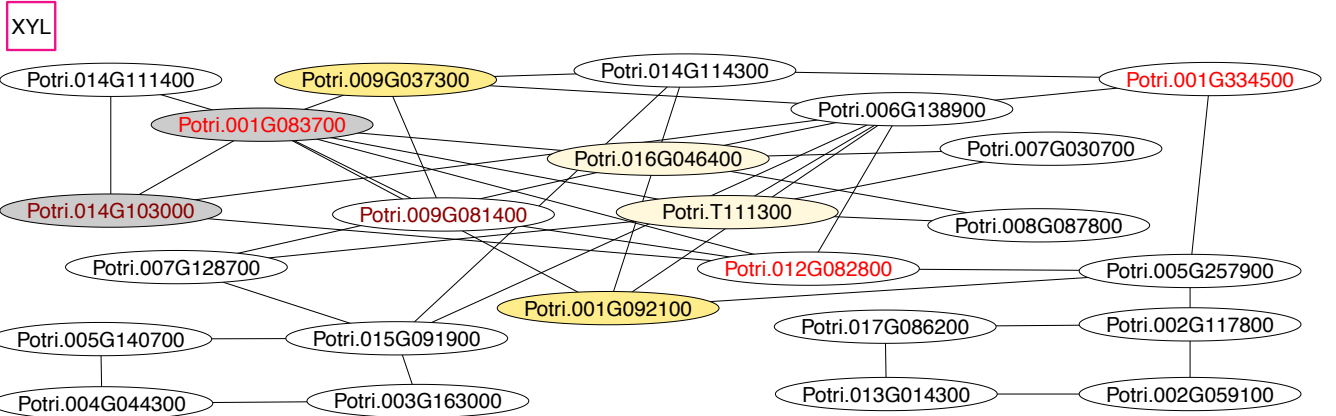
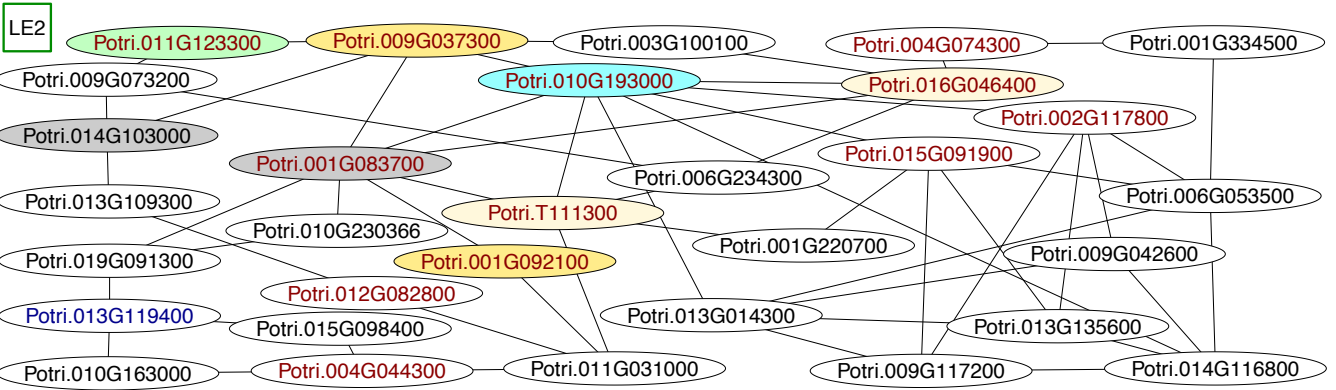
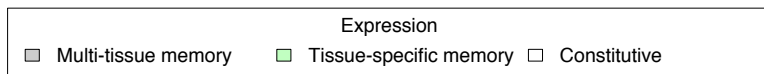
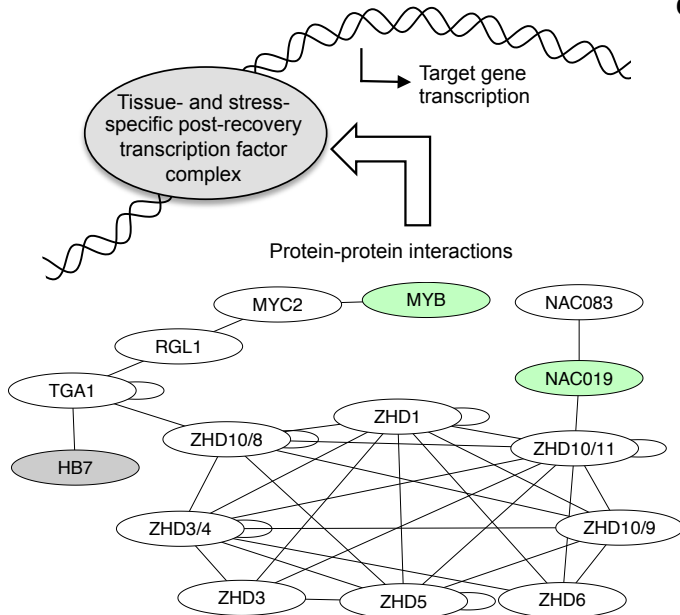
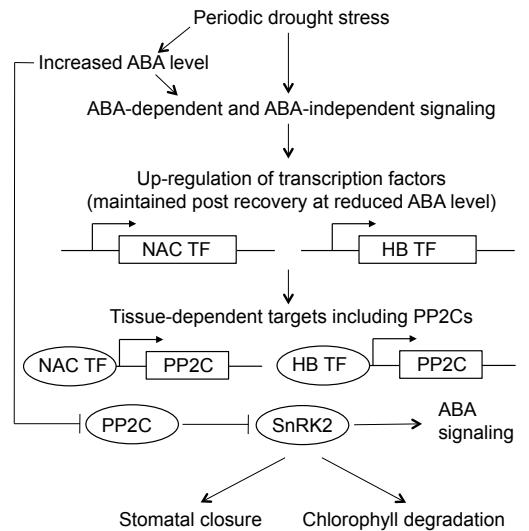
A**B****C**

Figure 8. Predicted regulatory stress-related memory processes in mature leaves (LE2) and developing xylem (XYL). (A) Core regulatory networks obtained by iteratively removing single-edge nodes from expression-based regulatory network predictions (Figure 7A). Node label colors refer to periodic stress-related expression patterns. Function annotation is shown for selected nodes discussed in the main text. Potri.010G193000 is a co-ortholog of the *Arabidopsis thaliana* MYB transcription factor AT5G05790, here abbreviated as MYB. (B) Model of possible transcription factor complex formation in stress-related memory derived from protein-protein interaction data in *Arabidopsis thaliana*. Gene names are taken from the orthology information in Phytozome. For some ZHD ortholog groups, different *Arabidopsis* genes (marked by an *Arabidopsis* ZHD identifier after the slash) constitute the best BLASTP matches of poplar genes. (C) Model suggesting physiological roles of protein phosphatases of type 2C (PP2Cs) and regulatory transcription factors in mature leaves during and after periodic stress.

Parsed Citations

Abdelgawad, H., Zinta, G., Hegab, M.M., Pandey, R., Asard, H., and Abuelsoud, W. (2016). High salinity induces different oxidative stress and antioxidant responses in maize seedlings organs. *Front. Plant Sci.* 7: 276.

Pubmed: [Author and Title](#)

Google Scholar: [Author Only Title Only Author and Title](#)

Abraham, P.E., Garcia, B.J., Gunter, L.E., Jawdy, S.S., Engle, N., Yang, X., Jacobson, D.A., Hettich, R.L., Tuskan, G.A., and Tschaplinski, T.J. (2018). Quantitative proteome profile of water deficit stress responses in eastern cottonwood (*Populus deltoides*) leaves. *PLoS One* 13: e0190019.

Pubmed: [Author and Title](#)

Google Scholar: [Author Only Title Only Author and Title](#)

Aibar, S., Gonzalez-Bias, C.B., Moerman, T., Huynh-Thu, V.A., Imrichova, H., Hulselmans, G., Rambow, F., Marine, J.C., Geurts, P., Aerts, J., et al. (2017). SCENIC: single-cell regulatory network inference and clustering. *Nat. Methods* 14: 1083-1086.

Pubmed: [Author and Title](#)

Google Scholar: [Author Only Title Only Author and Title](#)

Arabidopsis Interactome Mapping Consortium (2011). Evidence for network evolution in an Arabidopsis interactome map. *Science* 333: 601-607.

Pubmed: [Author and Title](#)

Google Scholar: [Author Only Title Only Author and Title](#)

Ariel, F.D., Manavella, P.A., Dezar, C.A., and Chan, R.L. (2007). The true story of the HD-Zip family. *Trends Plant Sci.* 12: 419-426.

Pubmed: [Author and Title](#)

Google Scholar: [Author Only Title Only Author and Title](#)

Aroca, R., Porcel, R., and Ruiz-Lozano, J.M. (2012). Regulation of root water uptake under abiotic stress conditions. *J. Exp. Bot.* 63: 43-57.

Pubmed: [Author and Title](#)

Google Scholar: [Author Only Title Only Author and Title](#)

Asensi-Fabado, M.A., Amtmann, A., and Perrella, G. (2017). Plant responses to abiotic stress: The chromatin context of transcriptional regulation. *Biochim. Biophys. Acta* 1860: 106-122.

Pubmed: [Author and Title](#)

Google Scholar: [Author Only Title Only Author and Title](#)

Auguie, B. (2017). gridExtra: Miscellaneous Functions for "Grid" Graphics.

Battaglia, M., Olvera-Carrillo, Y., Garcarrubio, A., Campos, F., and Covarrubias, A.A. (2008). The enigmatic LEA proteins and other hydrophilins. *Plant Physiol.* 148: 6-24.

Pubmed: [Author and Title](#)

Google Scholar: [Author Only Title Only Author and Title](#)

Berardini, T.Z., Reiser, L., Li, D., Mezheritsky, Y., Muller, R., Strait, E., and Huala, E. (2015). The Arabidopsis information resource: Making and mining the "gold standard" annotated reference plant genome. *Genesis* 53: 474-485.

Pubmed: [Author and Title](#)

Google Scholar: [Author Only Title Only Author and Title](#)

Bi, Z., Merl-Pham, J., Uehlein, N., Zimmer, I., Mühlhans, S., Aichler, M., Walch, A.K., Kaldenhoff, R., Palme, K., Schnitzler, J.P., et al. (2015). RNAi-mediated downregulation of poplar plasma membrane intrinsic proteins (PIPs) changes plasma membrane proteome composition and affects leaf physiology. *J. Proteomics* 128: 321-332.

Pubmed: [Author and Title](#)

Google Scholar: [Author Only Title Only Author and Title](#)

Bloemen, J., Vergeynst, L.L., Overlaet-Michiels, L., and Steppe, K. (2016). How important is woody tissue photosynthesis in poplar during drought stress? *Trees* 30: 63-72.

Pubmed: [Author and Title](#)

Google Scholar: [Author Only Title Only Author and Title](#)

Challa, K.R., Aggarwal, P., and Nath, U. (2016). Activation of YUCCA5 by the transcription factor TCP4 integrates developmental and environmental signals to promote hypocotyl elongation in Arabidopsis. *Plant Cell* 28: 2217-2130.

Pubmed: [Author and Title](#)

Google Scholar: [Author Only Title Only Author and Title](#)

Chen, J., Zhang, D., Zhang, C., Xia, X., Yin, W., and Tian, Q. (2015). A Putative PP2C-Encoding Gene Negatively Regulates ABA Signaling in *Populus euphratica*. *PLoS One* 10: e0139466.

Pubmed: [Author and Title](#)

Google Scholar: [Author Only Title Only Author and Title](#)

Crisp, P.A., Ganguly, D., Eichten, S.R., Borevitz, J.O., and Pogson, B.J. (2016). Reconsidering plant memory: Intersections between stress recovery, RNA turnover, and epigenetics. *Sci. Adv.* 2: e1501340.

Pubmed: [Author and Title](#)

Google Scholar: [Author Only Title Only Author and Title](#)

Csardi, G., and Nepusz, T. (2006). The igraph software package for complex network research. *InterJournal Complex Systems*: 1695.

Pubmed: [Author and Title](#)

Google Scholar: [Author Only Title Only Author and Title](#)

Ding, Y., Fromm, M., and Avramova, Z. (2012). Multiple exposures to drought 'train' transcriptional responses in *Arabidopsis*. *Nat. Commun.* 3: 740.

Pubmed: [Author and Title](#)

Google Scholar: [Author Only Title Only Author and Title](#)

Ding, Y., Liu, N., Virlouvet, L., Riethoven, J.J., Fromm, M., and Avramova, Z. (2013). Four distinct types of dehydration stress memory genes in *Arabidopsis thaliana*. *BMC Plant Biol.* 13: 229.

Pubmed: [Author and Title](#)

Google Scholar: [Author Only Title Only Author and Title](#)

Dong, C.J., and Liu, J.Y. (2010). The *Arabidopsis* EAR-motif-containing protein RAP2.1 functions as an active transcriptional repressor to keep stress responses under tight control. *BMC Plant Biol.* 10: 47.

Pubmed: [Author and Title](#)

Google Scholar: [Author Only Title Only Author and Title](#)

Dupeux, F., Antoni, R., Betz, K., Santiago, J., Gonzalez-Guzman, M., Rodriguez, L., Rubio, S., Park, S.Y., Cutler, S.R., Rodriguez, P.L., et al. (2011). Modulation of abscisic acid signaling in vivo by an engineered receptor-insensitive protein phosphatase type 2C allele. *Plant Physiol.* 156: 106-116.

Pubmed: [Author and Title](#)

Google Scholar: [Author Only Title Only Author and Title](#)

Dusa, A. (2018). venn: Draw Venn Diagrams.

Fleta-Soriano, E. and Munne-Bosch, S. (2016). Stress Memory and the inevitable effects of drought: a physiological perspective. *Front. Plant Sci.* 7: 143.

Pubmed: [Author and Title](#)

Google Scholar: [Author Only Title Only Author and Title](#)

Fox, J., and Weisberg, S. (2011). An R Companion to Applied Regression (Sage).

Fuchs, S., Grill, E., Meskiene, I., and Schweighofer, A. (2013). Type 2C protein phosphatases in plants. *FEBS J.* 280: 681-693.

Pubmed: [Author and Title](#)

Google Scholar: [Author Only Title Only Author and Title](#)

Fujii, H., Verslues, P.E., and Zhu, J.K. (2011). *Arabidopsis* decuple mutant reveals the importance of SnRK2 kinases in osmotic stress responses in vivo. *Proc. Natl. Acad. Sci. U. S. A.* 108: 1717-1722.

Pubmed: [Author and Title](#)

Google Scholar: [Author Only Title Only Author and Title](#)

Gansner, E.R., and North, S.C. (2000). An open graph visualization system and its applications to software engineering. *SOFTWARE - PRACTICE AND EXPERIENCE* 30: 1203-1233.

Pubmed: [Author and Title](#)

Google Scholar: [Author Only Title Only Author and Title](#)

Gao, S., Gao, J., Zhu, X., Song, Y., Li, Z., Ren, G., Zhou, X., and Kuai, B. (2016). ABF2, ABF3, and ABF4 promote ABA-mediated chlorophyll degradation and leaf senescence by transcriptional activation of chlorophyll catabolic genes and senescence-associated genes in *Arabidopsis*. *Mol Plant* 9: 1272-1285.

Pubmed: [Author and Title](#)

Google Scholar: [Author Only Title Only Author and Title](#)

Gonzalez, I., Le Cao, K.A., and Dejean, S. (2011). mixOmics: Omics data integration project.

Goodstein, D.M., Shu, S., Howson, R., Neupane, R., Hayes, R.D., Fazo, J., Mitros, T., Dirks, W., Hellsten, U., Putnam, N., et al. (2012). *Phytozome*: a comparative platform for green plant genomics. *Nucleic Acids Res.* 40: D1178-1186.

Pubmed: [Author and Title](#)

Google Scholar: [Author Only Title Only Author and Title](#)

Hagedorn, F., Joseph, J., Peter, M., Luster, J., Pritsch, K., Geppert, U., Kerner, R., Molinier, V., Egli, S., Schaub, M., et al. (2016). Recovery of trees from drought depends on belowground sink control. *Nat. Plants* 2: 16111.

Pubmed: [Author and Title](#)

Google Scholar: [Author Only Title Only Author and Title](#)

Harfouche, A., Meilan, R., and Altman, A. (2014). Molecular and physiological responses to abiotic stress in forest trees and their relevance to tree improvement. *Tree Physiol* 34: 1181-1198.

Pubmed: [Author and Title](#)

Google Scholar: [Author Only Title Only Author and Title](#)

Hilker, M., Schwachtje, J., Baier, M., Balazadeh, S., Baurle, I., Geiselhardt, S., Hinch, D.K., Kunze, R., Mueller-Roeber, B., Rillig, M.C., et al. (2016). Priming and memory of stress responses in organisms lacking a nervous system. *Biol. Rev. Camb. Philos. Soc.* 91: 1118-1133.

- Pubmed: [Author and Title](#)
Google Scholar: [Author Only Title Only Author and Title](#)
- Hjellström, M., Olsson, A.S.B., Engström, O., and Söderman, E.M. (2003). Constitutive expression of the water deficit-inducible homeobox gene ATHB7 in transgenic Arabidopsis causes a suppression of stem elongation growth. *Plant Cell Environ.* 26: 1127-1136.
Pubmed: [Author and Title](#)
Google Scholar: [Author Only Title Only Author and Title](#)
- Huynh-Thu, V.A., Irrthum, A., Wehenkel, L., and Geurts, P. (2010). Inferring regulatory networks from expression data using tree-based methods. *PLoS One* 5.
Pubmed: [Author and Title](#)
Google Scholar: [Author Only Title Only Author and Title](#)
- International Barley Genome Sequencing Consortium, Mayer, K.F., Waugh, R., Brown, J.W., Schulman, A., Langridge, P., Platzer, M., Fincher, G.B., Muehlbauer, G.J., Sato, K., et al. (2012). A physical, genetic and functional sequence assembly of the barley genome. *Nature* 491: 711-716.
Pubmed: [Author and Title](#)
Google Scholar: [Author Only Title Only Author and Title](#)
- IPCC (2014). Near-term Climate Change: Projections and Predictability. In *Climate Change 2013: The Physical Science Basis. Contribution of Working Group I to the Fifth Assessment Report of the Intergovernmental Panel on Climate Change*, T.F. Stocker, D. Qin, G.K. Plattner, M. Tignor, S.K. Allen, J. Boschung, A. Nauels, Y. Xia, B. V., and P.M. Midgley, eds. (Cambridge: Cambridge University Press).
Pubmed: [Author and Title](#)
Google Scholar: [Author Only Title Only Author and Title](#)
- Jin, J., Zhang, H., Kong, L., Gao, G., and Luo, J. (2014). PlantTFDB 3.0: a portal for the functional and evolutionary study of plant transcription factors. *Nucleic Acids Res.* 42: D1182-1187.
Pubmed: [Author and Title](#)
Google Scholar: [Author Only Title Only Author and Title](#)
- Jud, W., Vanzo, E., Li, Z., Ghirardo, A., Zimmer, I., Sharkey, T.D., Hansel, A., and Schnitzler, J.P. (2016). Effects of heat and drought stress on post-illumination bursts of volatile organic compounds in isoprene-emitting and non-emitting poplar. *Plant Cell Environ.* 39: 1204-1215.
Pubmed: [Author and Title](#)
Google Scholar: [Author Only Title Only Author and Title](#)
- Kim, D., Pertea, G., Trapnell, C., Pimentel, H., Kelley, R., and Salzberg, S.L. (2013). TopHat2: accurate alignment of transcriptomes in the presence of insertions, deletions and gene fusions. *Genome Biol.* 14: R36.
Pubmed: [Author and Title](#)
Google Scholar: [Author Only Title Only Author and Title](#)
- Kim, M., Lee, U., Small, I., des Francs-Small, C.C., and Vierling, E. (2012). Mutations in an Arabidopsis mitochondrial transcription termination factor-related protein enhance thermotolerance in the absence of the major molecular chaperone HSP101. *Plant Cell* 24: 3349-3365.
Pubmed: [Author and Title](#)
Google Scholar: [Author Only Title Only Author and Title](#)
- Kolde, R. (2018). pheatmap: Pretty Heatmaps.**
- Kotak, S., Larkindale, J., Lee, U., von Koskull-Doring, P., Vierling, E., and Scharf, K.D. (2007). Complexity of the heat stress response in plants. *Curr. Opin. Plant Biol.* 10: 310-316.
Pubmed: [Author and Title](#)
Google Scholar: [Author Only Title Only Author and Title](#)
- Kulik, A., Wawer, I., Krzywinska, E., Bucholc, M., and Dobrowolska, G. (2011). SnRK2 protein kinases—key regulators of plant response to abiotic stresses. *OMICS* 15: 859-872.
Pubmed: [Author and Title](#)
Google Scholar: [Author Only Title Only Author and Title](#)
- Länke, J., Brzezinka, K., Altmann, S., and Bäurle, I. (2016). A hit-and-run heat shock factor governs sustained histone methylation and transcriptional stress memory. *EMBO J.* 35: 162-175.
Pubmed: [Author and Title](#)
Google Scholar: [Author Only Title Only Author and Title](#)
- Langfelder, P., and Horvath, S. (2007). Eigengene networks for studying the relationships between co-expression modules. *BMC Syst. Biol.* 1: 54.
Pubmed: [Author and Title](#)
Google Scholar: [Author Only Title Only Author and Title](#)
- Langfelder, P., and Horvath, S. (2008). WGCNA: an R package for weighted correlation network analysis. *BMC Bioinformatics* 9: 559.
Pubmed: [Author and Title](#)
Google Scholar: [Author Only Title Only Author and Title](#)
- Langfelder, P., and Horvath, S. (2012). Fast R Functions for Robust Correlations and Hierarchical Clustering. *J Stat Softw* 46.

- Pubmed: [Author and Title](#)
Google Scholar: [Author Only Title Only Author and Title](#)
- Langfelder, P., Zhang, B., and Horvath, S. (2008).** Defining clusters from a hierarchical cluster tree: the dynamic tree cut package for R. *Bioinformatics* 24: 719-720.
Pubmed: [Author and Title](#)
Google Scholar: [Author Only Title Only Author and Title](#)
- Le Cao, K.A., Gonzalez, I., and Dejean, S. (2009).** integrOmics: an R package to unravel relationships between two omics datasets. *Bioinformatics* 25: 2855-2856.
Pubmed: [Author and Title](#)
Google Scholar: [Author Only Title Only Author and Title](#)
- Leonhardt, N., Kwak, J.M., Robert, N., Waner, D., Leonhardt, G., and Schroeder, J.I. (2004).** Microarray expression analyses of Arabidopsis guard cells and isolation of a recessive abscisic acid hypersensitive protein phosphatase 2C mutant. *Plant Cell* 16: 596-615.
Pubmed: [Author and Title](#)
Google Scholar: [Author Only Title Only Author and Title](#)
- Leplé, J.C., Brasileiro, A.C., Michel, M.F., Delmotte, F., and Jouanin, L. (1992).** Transgenic poplars: expression of chimeric genes using four different constructs. *Plant Cell Rep.* 11: 137-141.
Pubmed: [Author and Title](#)
Google Scholar: [Author Only Title Only Author and Title](#)
- Li, S. (2014).** Redox modulation matters: emerging functions for glutaredoxins in plant development and stress responses. *Plants (Basel)* 3: 559-582.
Pubmed: [Author and Title](#)
Google Scholar: [Author Only Title Only Author and Title](#)
- Lippold, F., vom Dorp, K., Abraham, M., Holzl, G., Wewer, V., Yilmaz, J.L., Lager, I., Montandon, C., Besagni, C., Kessler, F., et al. (2012).** Fatty acid phytyl ester synthesis in chloroplasts of Arabidopsis. *Plant Cell* 24: 2001-2014.
Pubmed: [Author and Title](#)
Google Scholar: [Author Only Title Only Author and Title](#)
- Liu, N., Staswick, P.E., and Avramova, Z. (2016).** Memory responses of jasmonic acid-associated Arabidopsis genes to a repeated dehydration stress. *Plant Cell Environ.* 39: 2515-2529.
Pubmed: [Author and Title](#)
Google Scholar: [Author Only Title Only Author and Title](#)
- Love, M.I., Huber, W., and Anders, S. (2014).** Moderated estimation of fold change and dispersion for RNA-seq data with DESeq2. *Genome Biol.* 15: 550.
Pubmed: [Author and Title](#)
Google Scholar: [Author Only Title Only Author and Title](#)
- Mi, H., Huang, X., Muruganujan, A., Tang, H., Mills, C., Kang, D., and Thomas, P.D. (2017).** PANTHER version 11: expanded annotation data from Gene Ontology and Reactome pathways, and data analysis tool enhancements. *Nucleic Acids Res.* 45: D183-D189.
Pubmed: [Author and Title](#)
Google Scholar: [Author Only Title Only Author and Title](#)
- Nakashima, K., Fujita, Y., Kanamori, N., Katagiri, T., Umezawa, T., Kidokoro, S., Maruyama, K., Yoshida, T., Ishiyama, K., Kobayashi, M., et al. (2009).** Three Arabidopsis SnRK2 protein kinases, SRK2D/SnRK2.2, SRK2E/SnRK2.6/OST1 and SRK2I/SnRK2.3, involved in ABA signaling are essential for the control of seed development and dormancy. *Plant Cell Physiol.* 50: 1345-1363.
Pubmed: [Author and Title](#)
Google Scholar: [Author Only Title Only Author and Title](#)
- Nakashima, K., Yamaguchi-Shinozaki, K., and Shinozaki, K. (2014).** The transcriptional regulatory network in the drought response and its crosstalk in abiotic stress responses including drought, cold, and heat. *Front. Plant Sci.* 5: 170.
Pubmed: [Author and Title](#)
Google Scholar: [Author Only Title Only Author and Title](#)
- Olvera-Carrillo, Y., Campos, F., Reyes, J.L., Garcarrubio, A., and Covarrubias, AA (2010).** Functional analysis of the group 4 late embryogenesis abundant proteins reveals their relevance in the adaptive response during water deficit in Arabidopsis. *Plant Physiol.* 154: 373-390.
Pubmed: [Author and Title](#)
Google Scholar: [Author Only Title Only Author and Title](#)
- Osakabe, Y., Osakabe, K., Shinozaki, K., and Tran, L.S. (2014).** Response of plants to water stress. *Front. Plant Sci.* 5: 86.
Pubmed: [Author and Title](#)
Google Scholar: [Author Only Title Only Author and Title](#)
- Paul, S., Wildhagen, H., Janz, D., and Polle, A. (2018).** Drought effects on the tissue- and cell-specific cytokinin activity in poplar. *AoB Plants* 10: plx067.
Pubmed: [Author and Title](#)
Google Scholar: [Author Only Title Only Author and Title](#)

Pertea, M., Pertea, G.M., Antonescu, C.M., Chang, T.C., Mendell, J.T., and Salzberg, S.L. (2015). StringTie enables improved reconstruction of a transcriptome from RNA-seq reads. *Nat. Biotechnol.* 33: 290-295.

Pubmed: [Author and Title](#)

Google Scholar: [Author Only](#) [Title Only](#) [Author and Title](#)

Pfanz, H., Aschan, G., Langenfeld-Heyser, R., Wittmann, C., and Loose, M. (2002). Ecology and ecophysiology of tree stems: corticular and wood photosynthesis. *Naturwissenschaften* 89: 147-162.

Pubmed: [Author and Title](#)

Google Scholar: [Author Only](#) [Title Only](#) [Author and Title](#)

R Core Team (2018). R: A Language and Environment for Statistical Computing.

Re, D.A., Capella, M., Bonaventure, G., and Chan, R.L. (2014). *Arabidopsis* AtHB7 and AtHB12 evolved divergently to fine tune processes associated with growth and responses to water stress. *BMC Plant Biol.* 14: 150.

Pubmed: [Author and Title](#)

Google Scholar: [Author Only](#) [Title Only](#) [Author and Title](#)

Samol, I., Shapiguzov, A., Ingelsson, B., Fucile, G., Crevecoeur, M., Vener, A.V., Rochaix, J.D., and Goldschmidt-Clermont, M. (2012). Identification of a photosystem II phosphatase involved in light acclimation in *Arabidopsis*. *Plant Cell* 24: 2596-2609.

Pubmed: [Author and Title](#)

Google Scholar: [Author Only](#) [Title Only](#) [Author and Title](#)

Sani, E., Herzyk, P., Perrella, G., Colot, V., and Amtmann, A. (2013). Hyperosmotic priming of *Arabidopsis* seedlings establishes a long-term somatic memory accompanied by specific changes of the epigenome. *Genome Biol.* 14: R59.

Pubmed: [Author and Title](#)

Google Scholar: [Author Only](#) [Title Only](#) [Author and Title](#)

Schäfer, J., and Strimmer, K. (2005). A shrinkage approach to large-scale covariance matrix estimation and implications for functional genomics. *Stat. Appl. Genet. Mol. Biol.* 4: Article32.

Pubmed: [Author and Title](#)

Google Scholar: [Author Only](#) [Title Only](#) [Author and Title](#)

Scholander, P.F., Bradstreet, E.D., Hemmingsen, E.A., and Hammel, H.T. (1965). Sap pressure in vascular plants: negative hydrostatic pressure can be measured in plants. *Science* 148: 339-346.

Pubmed: [Author and Title](#)

Google Scholar: [Author Only](#) [Title Only](#) [Author and Title](#)

Shinozaki, K., and Yamaguchi-Shinozaki, K. (2007). Gene networks involved in drought stress response and tolerance. *J. Exp. Bot.* 58: 221-227.

Pubmed: [Author and Title](#)

Google Scholar: [Author Only](#) [Title Only](#) [Author and Title](#)

Singh, D., and Laxmi, A. (2015). Transcriptional regulation of drought response: a tortuous network of transcriptional factors. *Front. Plant Sci.* 6: 895.

Pubmed: [Author and Title](#)

Google Scholar: [Author Only](#) [Title Only](#) [Author and Title](#)

Söderman, E., Mattsson, J., and Engström, P. (1996). The *Arabidopsis* homeobox gene ATHB-7 is induced by water deficit and by abscisic acid. *Plant J.* 10: 375-381.

Pubmed: [Author and Title](#)

Google Scholar: [Author Only](#) [Title Only](#) [Author and Title](#)

Soy, J., Leivar, P., Gonzalez-Schain, N., Sentandreu, M., Prat, S., Quail, P.H., and Monte, E. (2012). Phytochrome-imposed oscillations in PIF3 protein abundance regulate hypocotyl growth under diurnal light/dark conditions in *Arabidopsis*. *Plant J.* 71: 390-401.

Pubmed: [Author and Title](#)

Google Scholar: [Author Only](#) [Title Only](#) [Author and Title](#)

Sun, X., Wang, C., Xiang, N., Li, X., Yang, S., Du, J., Yang, Y., and Yang, Y. (2017). Activation of secondary cell wall biosynthesis by miR319-targeted TCP4 transcription factor. *Plant Biotechnol. J.* 15: 1284-1294.

Pubmed: [Author and Title](#)

Google Scholar: [Author Only](#) [Title Only](#) [Author and Title](#)

Sundell, D., Street, N.R., Kumar, M., Mellerowicz, E.J., Kucukoglu, M., Johnsson, C., Kumar, V., Mannapperuma, C., Delhomme, N., Nilsson, O., et al. (2017). AspWood: High-spatial-resolution transcriptome profiles reveal uncharacterized modularity of wood formation in *Populus tremula*. *Plant Cell* 29: 1585-1604.

Pubmed: [Author and Title](#)

Google Scholar: [Author Only](#) [Title Only](#) [Author and Title](#)

Tan, Q.K., and Irish, V.F. (2006). The *Arabidopsis* zinc finger-homeodomain genes encode proteins with unique biochemical properties that are coordinately expressed during floral development. *Plant Physiol.* 140: 1095-1108.

Pubmed: [Author and Title](#)

Google Scholar: [Author Only](#) [Title Only](#) [Author and Title](#)

Taylor, G. (2002). *Populus*: arabidopsis for forestry. Do we need a model tree? *Ann. Bot.* 90: 681-689.

Pubmed: [Author and Title](#)

Google Scholar: [Author Only](#) [Title Only](#) [Author and Title](#)

Thiel, S., Döhring, T., Köfferlein, M., Kosak, A., Martin, P., and Seidlitz, H.K. (1996) A phytotron for plant stress research: How far can artificial lighting compare to natural sunlight? J. Plant Physiol. 148: 456–463.

Pubmed: [Author and Title](#)

Google Scholar: [Author Only](#) [Title Only](#) [Author and Title](#)

Tischer, S.V., Wunschel, C., Papacek, M., Kleigrewe, K., Hofmann, T., Christmann, A., and Grill, E. (2017). Combinatorial interaction network of abscisic acid receptors and coreceptors from *Arabidopsis thaliana*. Proc. Natl. Acad. Sci. U. S. A 114: 10280-10285.

Pubmed: [Author and Title](#)

Google Scholar: [Author Only](#) [Title Only](#) [Author and Title](#)

Tran, L.S., Nakashima, K., Sakuma, Y., Osakabe, Y., Qin, F., Simpson, S.D., Maruyama, K., Fujita, Y., Shinozaki, K., and Yamaguchi-Shinozaki, K. (2007). Co-expression of the stress-inducible zinc finger homeodomain ZFHD1 and NAC transcription factors enhances expression of the ERD1 gene in *Arabidopsis*. Plant J. 49: 46-63.

Pubmed: [Author and Title](#)

Google Scholar: [Author Only](#) [Title Only](#) [Author and Title](#)

Tran, L.S., Nakashima, K., Sakuma, Y., Simpson, S.D., Fujita, Y., Maruyama, K., Fujita, M., Seki, M., Shinozaki, K., and Yamaguchi-Shinozaki, K. (2004). Isolation and functional analysis of *Arabidopsis* stress-inducible NAC transcription factors that bind to a drought-responsive cis-element in the early responsive to dehydration stress 1 promoter. Plant Cell 16: 2481-2498.

Pubmed: [Author and Title](#)

Google Scholar: [Author Only](#) [Title Only](#) [Author and Title](#)

Tuskan, G.A., Difazio, S., Jansson, S., Bohlmann, J., Grigoriev, I., Hellsten, U., Putnam, N., Ralph, S., Rombauts, S., Salamov, A., et al. (2006). The genome of black cottonwood, *Populus trichocarpa* (Torr. & Gray). Science 313: 1596-1604.

Pubmed: [Author and Title](#)

Google Scholar: [Author Only](#) [Title Only](#) [Author and Title](#)

Valdés, A.E., Overnäs, E., Johansson, H., Rada-Iglesias, A., and Engström, P. (2012). The homeodomain-leucine zipper (HD-Zip) class I transcription factors ATHB7 and ATHB12 modulate abscisic acid signalling by regulating protein phosphatase 2C and abscisic acid receptor gene activities. Plant Mol. Biol. 80: 405-418.

Pubmed: [Author and Title](#)

Google Scholar: [Author Only](#) [Title Only](#) [Author and Title](#)

Vanzo, E., Jud, W., Li, Z., Albert, A., Domagalska, M.A., Ghirardo, A., Niederbacher, B., Frenzel, J., Beemster, G.T., Asard, H., et al. (2015). Facing the future: effects of short-term climate extremes on isoprene-emitting and non-emitting poplar. Plant Physiol. 169: 560-575.

Pubmed: [Author and Title](#)

Google Scholar: [Author Only](#) [Title Only](#) [Author and Title](#)

von Caemmerer, S., and Farquhar, G.D. (1981). Some relationships between the biochemistry of photosynthesis and the gas exchange of leaves. Planta 153: 376-387.

Pubmed: [Author and Title](#)

Google Scholar: [Author Only](#) [Title Only](#) [Author and Title](#)

Wang, L., Hua, D., He, J., Duan, Y., Chen, Z., Hong, X., and Gong, Z. (2011). Auxin Response Factor2 (ARF2) and its regulated homeodomain gene HB33 mediate abscisic acid response in *Arabidopsis*. PLoS Genet. 7: e1002172.

Pubmed: [Author and Title](#)

Google Scholar: [Author Only](#) [Title Only](#) [Author and Title](#)

Wang, X., Vignjevic, M., Jiang, D., Jacobsen, S., and Wollenweber, B. (2014). Improved tolerance to drought stress after anthesis due to priming before anthesis in wheat (*Triticum aestivum* L.) var. Vinjett. J. Exp. Bot. 65: 6441-6456.

Pubmed: [Author and Title](#)

Google Scholar: [Author Only](#) [Title Only](#) [Author and Title](#)

Warnes, G.R., Bolker, B., Bonebakker, L., Gentleman, R., Huber, W., Liaw, A., Lumley, T., Maechler, M., Magnusson, A., Moeller, S., et al. (2016). ggplots: Various R Programming Tools for Plotting Data.

Wickham, H. (2009). ggplot2: Elegant Graphics for Data Analysis (Springer-Verlag New York).

Pubmed: [Author and Title](#)

Google Scholar: [Author Only](#) [Title Only](#) [Author and Title](#)

Wildhagen, H., Paul, S., Allwright, M., Smith, H.K., Malinowska, M., Schnabel, S.K., Paulo, M.J., Cattonaro, F., Vendramin, V., Scalabrin, S., et al. (2018). Genes and gene clusters related to genotype and drought-induced variation in saccharification potential, lignin content and wood anatomical traits in *Populus nigra*. Tree Physiol 38: 320-339.

Pubmed: [Author and Title](#)

Google Scholar: [Author Only](#) [Title Only](#) [Author and Title](#)

Xu, Z., Zhou, G., and Shimizu, H. (2010). Plant responses to drought and rewatering. Plant Signal. Behav. 5: 649-654.

Pubmed: [Author and Title](#)

Google Scholar: [Author Only](#) [Title Only](#) [Author and Title](#)

Yao, W., Zhang, X., Zhou, B., Zhao, K., Li, R., and Jiang, T. (2017). Expression pattern of ERF gene family under multiple abiotic stresses in *Populus simonii* x *P. nigra*. Front. Plant Sci. 8: 181.

Pubmed: [Author and Title](#)

Google Scholar: [Author Only](#) [Title Only](#) [Author and Title](#)

Yazaki, J., Galli, M., Kim, A.Y., Nito, K., Aleman, F., Chang, K.N., Carvunis, A.R., Quan, R., Nguyen, H., Song, L., et al. (2016). Mapping transcription factor interactome networks using HaloTag protein arrays. Proc. Natl. Acad. Sci. U. S. A. 113: E4238-4247.

Pubmed: [Author and Title](#)

Google Scholar: [Author Only](#) [Title Only](#) [Author and Title](#)

Yu, J., Yang, L., Liu, X., Tang, R., Wang, Y., Ge, H., Wu, M., Zhang, J., Zhao, F., Luan, S., et al. (2016). Overexpression of poplar pyrabactin resistance-like abscisic acid receptors promotes abscisic acid sensitivity and drought resistance in transgenic Arabidopsis. PLoS One 11: e0168040.

Pubmed: [Author and Title](#)

Google Scholar: [Author Only](#) [Title Only](#) [Author and Title](#)

Zhang, K., and Gan, S.S. (2012). An abscisic acid-AtNAP transcription factor-SAG113 protein phosphatase 2C regulatory chain for controlling dehydration in senescing Arabidopsis leaves. Plant Physiol. 158: 961-969.

Pubmed: [Author and Title](#)

Google Scholar: [Author Only](#) [Title Only](#) [Author and Title](#)

Zhong, S., Shi, H., Xue, C., Wang, L., Xi, Y., Li, J., Quail, P.H., Deng, X.W., and Guo, H. (2012). A molecular framework of light-controlled phytohormone action in Arabidopsis. Curr. Biol. 22: 1530-1535.

Pubmed: [Author and Title](#)

Google Scholar: [Author Only](#) [Title Only](#) [Author and Title](#)

The systems architecture of molecular memory in poplar after abiotic stress

Elisabeth Georgii, Karl G Kugler, Matthias Pfeifer, Elisa Vanzo, Katja Block, Malgorzata A. Domagalska, Werner Jud, Hamada AbdElgawad, Han Asard, Richard Reinhardt, Armin Hansel, Manuel Spannagl, Anton R. Schaeffner, Klaus Palme, Klaus Mayer and Joerg-Peter Schnitzler
Plant Cell; originally published online January 31, 2019;
DOI 10.1105/tpc.18.00431

This information is current as of February 28, 2019

Supplemental Data	/content/suppl/2019/01/31/tpc.18.00431.DC1.html /content/suppl/2019/02/01/tpc.18.00431.DC2.html
Permissions	https://www.copyright.com/ccc/openurl.do?sid=pd_hw1532298X&issn=1532298X&WT.mc_id=pd_hw1532298X
eTOCs	Sign up for eTOCs at: http://www.plantcell.org/cgi/alerts/ctmain
CiteTrack Alerts	Sign up for CiteTrack Alerts at: http://www.plantcell.org/cgi/alerts/ctmain
Subscription Information	Subscription Information for <i>The Plant Cell</i> and <i>Plant Physiology</i> is available at: http://www.aspb.org/publications/subscriptions.cfm